

Plasma-based techniques for clean and efficient hydrogen generation: A comprehensive review

Sima ealanloo ^a, Fatemeh Ahmadinouri ^{a, *}, Parviz Parvin ^a

^a Department of Energy Engineering and Physics, Amirkabir University of Technology (Tehran Polytechnic), Tehran, Iran.

Keywords

Hydrogen generation
Methane reforming
Hydrocarbon conversion
Clean energy

Article Info

DOI: [10.22060/aest.2026.25852.1006](https://doi.org/10.22060/aest.2026.25852.1006)

Received date: 5 March 2026

Accepted date 29 March 2026

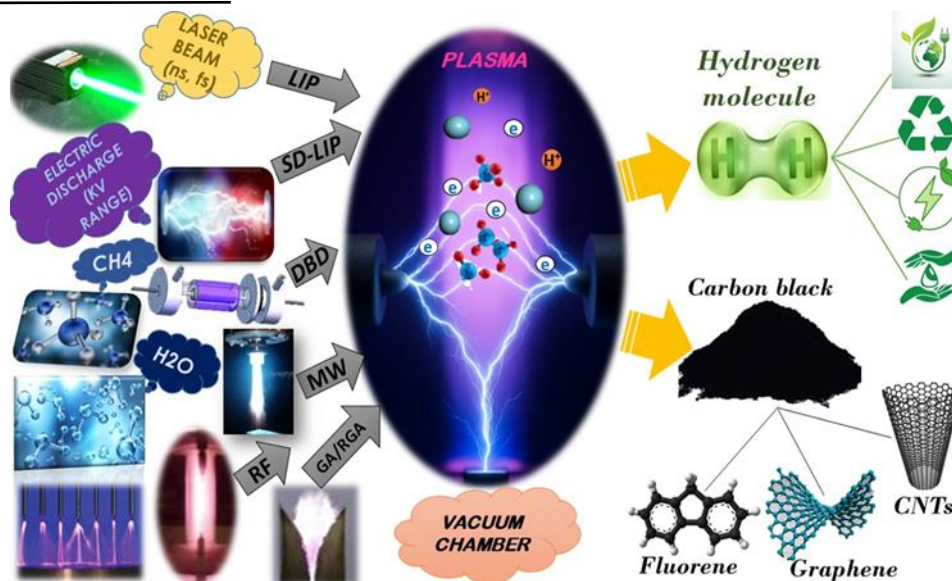
Published date 1 April 2026

* Corresponding author:
Parvin@aut.ac.ir

Abstract

Hydrogen is widely regarded as a promising clean energy carrier because of its high energy density and carbon-free utilization. This review presents a comprehensive overview of plasma-based techniques for hydrogen generation from water, methane, and other hydrocarbons, with emphasis on laser-induced plasma (LIP), spark discharge-assisted laser-induced plasma (SD-LIP), dielectric barrier discharge (DBD), corona discharge, microwave (MW) plasma, radio-frequency (RF) plasma, and glow/abnormal glow (GA/RGA) discharge systems. These methods provide highly reactive environments that promote molecular dissociation and hydrogen formation under relatively mild conditions. Particular attention is given to hybrid laser–spark approaches, which can enhance plasma density, prolong plasma lifetime, improve conversion efficiency, and reduce energy consumption. The review also compares the main plasma configurations in terms of operating principles, hydrogen yield, efficiency, and practical applicability. Overall, plasma-based routes show strong potential as flexible and sustainable alternatives for next-generation hydrogen generation.

Graphical Abstract



1. Introduction

The widespread utilization of hydrocarbon-based fuels during the twentieth century has significantly contributed to environmental pollution and global climate-related concerns. Consequently, the increasing demand for sustainable energy alternatives in recent decades has stimulated the development of numerous renewable energy strategies. In this context, hydrogen has emerged as a clean energy carrier with characteristics that make it a promising substitute for conventional fuels across a broad range of energy applications [1]. Hydrogen-based energy systems provide significant opportunities for fuel-cell technologies and a variety of other energy-related applications. When utilized in conjunction with fuel cells, hydrogen can efficiently generate clean and sustainable electrical power. In addition, hydrogen serves as an important feedstock in the petrochemical industry, particularly for the production of ammonia, methanol, and other valuable chemical products [2]. Hydrogen also demonstrates considerable potential for use in heating applications, power generation systems, and transportation sectors. Furthermore, the demand for hydrogen is expected to increase significantly as clean-energy technologies become more widely adopted, particularly in mobile energy and transportation systems. According to projections by the Hydrogen Council, the number of hydrogen fuel-cell vehicles could reach approximately 10 million passenger cars and 500,000 trucks in the coming years [3]. Hydrogen offers several notable advantages, including high energy-conversion efficiency, carbon-free utilization, and flexibility in storage through various forms such as compressed gas, liquid hydrogen, and metal hydride-based systems [4]. At present, global hydrogen consumption is estimated to be approximately 95 million tonnes per year, where it functions both as an energy carrier and as a key reactant in the production of fuels and valuable chemicals, including gasoline, ammonia, methanol, and a wide range of other high-value products [5]. As a result, the advancement of environmentally friendly, efficient, and sustainable hydrogen production methods has become a major focus of research efforts worldwide.

Hydrogen production technologies can generally be classified according to the primary form of energy used to initiate and sustain the reaction process. Laser-based techniques utilize highly coherent and monochromatic photon energy to induce localized water splitting, photoelectrochemical excitation, or laser-generated plasma reactions, allowing precise control over both reaction kinetics and product selectivity. In contrast, non-laser methods typically depend on thermal energy, electrical potentials, or non-coherent radiation to promote reactions within the bulk medium. These fundamental differences influence energy-conversion efficiency, catalyst requirements, scalability, and thermodynamic performance. While laser-assisted approaches offer superior control over reaction pathways and localized energy delivery, their implementation on a continuous industrial scale remains challenging. Conversely, non-laser technologies are generally more mature from an industrial perspective but may suffer from lower photon utilization efficiencies or greater thermal and electrical energy consumption [6]. Within light- and laser-assisted hydrogen production technologies, a further classification can be established between discharge-based and non-discharge approaches, each characterized by distinct operating principles and advantages. According to recent studies on plasma-assisted water splitting (Cook et al., 2025), discharge-based methods utilize highly ionized reaction environments to promote molecular dissociation, often resulting in accelerated reaction rates and localized energy transfer. In contrast, non-discharge photonic techniques rely on the direct absorption of photons by catalytic materials and proceed without

the formation of plasma. This fundamental distinction leads to significant differences in reaction pathways, energy-transfer efficiency, catalyst design considerations, and the potential for large-scale implementation [7].

Discharge-based light and laser technologies constitute an important class of hydrogen production methods that utilize electrical discharges or laser-generated plasma phenomena to produce reactive species capable of dissociating chemical bonds in feedstock molecules. These techniques are founded on the principles of low-temperature plasma science, where energetic electrons promote the formation of radicals and electronically excited species that facilitate a wide range of chemical reactions and conversion processes [8]. Among these technologies, Laser-Induced Plasma (LIP) has attracted considerable interest as an emerging method for hydrogen production. When a high-energy laser beam is focused onto the surface of a target material, rapid heating results in melting and vaporization of the irradiated region. In addition, laser-induced stresses can cause the direct ejection of particles from the target through mechanical fragmentation processes [9]. This particle ejection may occur as a consequence of molten material splashing from the target surface [10] or as a result of explosive boiling phenomena induced by intense laser irradiation [11]. Despite significant progress in plasma-catalytic technologies, their broader implementation remains constrained by the relatively high power requirements and limited energy efficiency of these systems. Increasing the input power often results in excessive heating, which can promote coke formation and consequently reduce catalytic activity and conversion performance. Furthermore, operation at elevated pressures is frequently associated with reduced spark mobility, accelerating electrode erosion and ultimately shortening the operational lifetime of the system [12]. To overcome the intrinsic drawbacks associated with conventional plasma-catalyst systems, recent research has combined laser-induced plasma with catalyst-assisted spark discharge, leading to the emergence of the Spark Discharge Laser-Induced Plasma (SD-LIP) technique. In this hybrid system, the laser acts as an in situ cleaning source that continuously removes carbonaceous deposits from the catalyst surface, thereby minimizing catalyst deactivation. In addition, plasma reheating occurs through the inverse Bremsstrahlung process [13], which promotes the formation of highly energetic electrons and consequently increases the local electron density within the discharge region [14,15]. Ahmadinouri et al. investigated methane conversion in a spark discharge-assisted laser-induced plasma (SD-LIP) reactor integrated with a palladium catalyst and reported improved hydrogen production efficiency. Their results revealed that laser-induced electron injection significantly lowered the breakdown voltage and suppressed coke formation, while simultaneously enhancing carbon balance and overall energy-conversion efficiency. These findings demonstrate the potential of the SD-LIP hybrid electro-photocatalytic system as an effective approach for environmentally friendly hydrogen production from methane [16]. In another study, Ahmadinouri et al. examined hydrogen production from propane using a laser-triggered spark discharge (LTSD) system and reported a significant enhancement in conversion performance compared with conventional plasma-based methods. The authors observed higher hydrogen yields, substantially lower breakdown voltages, and reduced energy consumption. Additionally, the laser-assisted process provided in situ cleaning of the catalyst surface, which helped suppress soot accumulation and mitigate catalyst deactivation. These results indicate that LTSD represents a promising plasma-assisted technology for efficient and more sustainable hydrogen production from LPG-based hydrocarbons [17]. Fatemeh Ahmadinouri et al. studied the non-oxidative conversion of methane using a hybrid spark discharge-assisted laser-induced plasma (SD-LIP) system and reported a considerable improvement in methane dissociation relative to conventional plasma techniques. The synergistic interaction between the spark discharge and laser-induced plasma decreased both the breakdown voltage and the overall energy requirement, while continuously removing

carbonaceous deposits from the catalyst surface. As a result, coke accumulation and catalyst deactivation were effectively suppressed. Their findings identify SD-LIP as a controllable and energy-efficient plasma-assisted approach with strong potential for sustainable methane conversion and hydrogen production applications [18]. Ghasemi et al. evaluated the capability of laser-induced breakdown spectroscopy (LIBS) for differentiating malignant tissues from healthy tissues in various human organs. Their findings revealed that cancerous samples contained higher levels of trace elements, including Ca, Mg, and Na, and were associated with increased plasma temperatures and electron densities, suggesting the generation of more energetic plasmas in neoplastic tissues. The results demonstrate that LIBS is a rapid, cost-effective, and real-time spectroscopic method with considerable potential for clinical cancer detection and diagnostic applications [19]. Ghorbani et al. investigated methane decomposition in a controlled reaction chamber using a Q-switched Nd:YAG laser, where various metallic catalysts (Pd, Ni, Fe, and Cu) were ablated to generate transient laser-induced plasmas around catalyst nanoparticles. FTIR and GC measurements verified the effective dissociation of methane in the presence of metal-assisted LIP, leading to the formation of hydrogen together with heavier hydrocarbons such as propane, ethane, and ethylene. The distribution of reaction products was found to depend strongly on both the catalyst type and the characteristics of the generated plasma. The authors attributed the enhanced methane conversion to energetic electron collisions and surface catalytic reactions occurring on the nanoparticles, which promote adsorption and spillover phenomena, weaken C–H bonds, and facilitate recombination pathways leading to the formation of higher hydrocarbons [13]. Habibpour et al. developed a laboratory-built calibration-free spark-assisted LIBS (CF SA-LIBS) system for the rapid determination of gold fineness (karat). The setup combined a Q-switched Nd:YAG laser with a spark generator, demonstrating that the additional electrical discharge can reheat and sustain the plasma plume. As a result, the plasma temperature increased by approximately 20%, the plasma lifetime was prolonged by nearly six times, and the emission intensity was enhanced by up to one order of magnitude under low single-shot laser energies. Electron density was estimated from Stark-broadened spectral lines and incorporated into Saha–Eggert relations under local thermodynamic equilibrium (LTE) conditions to improve the accuracy of the calibration-free analysis. The proposed method achieved gold karat measurements with analytical errors below 0.5%, while single-shot SA-LIBS produced less material ablation and sample damage than conventional LIBS, highlighting its suitability for portable and minimally invasive purity assessment applications [14]. Moosakhani et al. examined molecular decomposition in various hydrocarbon environments (C1–C4) by ablating a palladium target with a Q-switched Nd:YAG laser inside a controlled chamber. The study monitored the influence of the surrounding atmosphere on the ablated Pd mass, reaction products, and key plasma characteristics, including electron density (N_e) and electron temperature (T_e). Their results showed that hydrocarbon atmospheres, particularly methane, generate more energetic plasmas than synthetic air. This behavior was primarily attributed to oxygen-free exothermic decomposition and recombination reactions, together with additional heating and hydrodynamic expansion caused by the released Pd nanoparticles, which prolong plasma activity for several hundred nanoseconds. However, these decomposition and recombination processes also lead to soot formation and deposition within the chamber. The amount of soot increased nonlinearly from C1 to C4 hydrocarbons, progressively attenuating subsequent laser pulses and reducing both the effective plasma temperature and the concentration of Pd nanoparticles. Therefore, the observed variations in ablation behavior and plasma properties were governed by the combined effects of exothermic heat release and, more significantly, soot-induced attenuation of the laser radiation [20]. As part of ongoing efforts to advance innovative energy-related technologies, Parvin et

al. employed laser-induced breakdown spectroscopy (LIBS) and laser-induced fluorescence (LIF) spectroscopy to investigate crude oil-saturated carbonate rock formations. Their study provided a detailed analysis of the elemental composition of the samples as well as the thermal behavior of crude oil constituents. The obtained results demonstrated the effectiveness of these spectroscopic techniques for the identification, characterization, and differentiation of various crude oil components [21]. Aggressive brain tumors, including glioblastoma multiforme (GBM) and oligodendroglioma (OG), remain challenging to diagnose accurately, particularly during the early stages of disease progression. Laser-induced breakdown spectroscopy (LIBS) has emerged as a promising minimally invasive diagnostic technique through the analysis of plasma emission spectra generated from biological tissue samples. In a recent study, Mohammadimatin et al. demonstrated that spark-assisted LIBS (SA-LIBS) significantly improves spectral intensity and plasma characteristics, including temperature, electron density, and ionization degree, compared with conventional LIBS systems. The enhanced analytical performance enabled effective differentiation between glioma-affected tissues and infiltrated healthy regions, while stronger ionic emissions from elements such as Mg II and Ca II were identified as valuable indicators for early-stage tumor classification and grading [22]. Corona discharge is another important discharge-based technology, characterized by the generation of a self-sustaining plasma region surrounding a sharp electrode when subjected to a sufficiently high applied voltage [23]. Corona discharges typically function at atmospheric pressure under non-equilibrium plasma conditions, where high-energy electrons initiate and sustain chemical reactions while the temperature of the bulk gas remains close to ambient conditions [24]. Corona discharge has been extensively explored as a non-thermal plasma technology for hydrogen production from a variety of feedstocks, including water vapor, methane, and dimethyl ether. Reported energy efficiencies vary considerably depending on the operating conditions and feedstock composition, ranging from approximately 8% in liquid-water-based systems to nearly 80% in processes utilizing steam with argon as a carrier gas [25]. Microwave (MW) plasma systems produce electrical discharges through the coupling of electromagnetic radiation in the gigahertz frequency range, most commonly at 2.45 GHz, into a gaseous medium, allowing stable plasma generation without the need for electrodes. One of the primary advantages of this approach is the relatively uniform distribution of deposited energy throughout the plasma volume, which reduces thermal gradients and contributes to a more homogeneous reaction environment. Furthermore, MW plasmas offer a high degree of control over important plasma characteristics, since parameters such as electron density, gas temperature, and power-transfer efficiency can be independently adjusted through changes in input power, operating pressure, gas flow conditions, and waveguide or cavity design [26]. Jasiński et al. [27–30] examined the application of atmospheric-pressure microwave plasma for hydrogen production through methane decomposition and reforming processes using both pure CH₄ and CH₄-containing gas mixtures. Their investigations revealed that this plasma configuration can achieve high methane conversion rates together with competitive hydrogen energy yields, without the need for additional catalysts or high-temperature reactor systems. These results highlight atmospheric-pressure MW plasma as an efficient and attractive alternative to other discharge-based technologies, including gliding arc reactors, plasmatrons, and electron-beam-assisted systems. Czyilkowski et al. [31] were the first to apply a combined microwave-plasma-assisted steam reforming process for hydrogen production from CH₄/CO₂ mixtures. Their study reported a hydrogen energy yield of 43 g(H₂)/kWh, a value that approaches the target established by the U.S. Department of Energy, which is 60 g(H₂)/kWh. These results demonstrate the potential of microwave plasma technology as an efficient route for hydrogen generation from methane-containing feedstocks. Radio Frequency (RF) discharge technology typically operates within the

frequency range of 1–100 MHz, generating plasma through oscillating electric fields that accelerate electrons and sustain ionization while keeping the bulk gas temperature relatively low [32]. RF plasmas are distinguished by their capability to generate large, spatially uniform plasma volumes under non-equilibrium conditions, where the electron temperature is significantly higher than the temperature of neutral gas species ($T_e \gg T_{\text{gas}}$). This unique characteristic makes RF plasma systems particularly attractive for hydrogen production from a variety of carbon-based feedstocks [33]. Approximately two decades after the discovery of ozone by Christian Friedrich Schönbein in 1839, Siemens introduced a highly localized and transient non-thermal plasma operating at atmospheric pressure, which he referred to as a “silent discharge.” This discharge configuration is now widely known as dielectric barrier discharge (DBD) [34]. Owing to several advantageous characteristics, DBD has received considerable attention in recent years. These advantages include the generation of a broad range of chemically reactive species under ambient conditions, relatively uniform discharge distribution, high electron density, and favorable operating conditions for plasma-assisted chemical processes [35].

Gliding arc discharges offer a readily controllable energy source that can replace conventional high-temperature thermal processes with lower-energy cold plasma technologies in a variety of engineering and environmental applications [36]. The gliding arc in tornado (GAT) configuration employs a tangential reverse vortex flow that causes the arc column to rotate around the axis of the cylindrical reactor. This design promotes more uniform treatment of the process gas and provides a substantially longer residence time for reactive species compared with conventional gliding arc reactors based on flat-electrode geometries [37]. Rotating gliding arc (RGA) plasma is generally classified as a warm plasma because it exhibits characteristics of both thermal and non-thermal plasmas. It is characterized by relatively high electron density and electron energy while maintaining a moderate gas temperature, a combination that is advantageous for efficient hydrogen production and enhanced process productivity [38]. Owing to these favorable properties, RGA plasma has been employed by several researchers for hydrogen generation through methane reforming processes [39–41]. Natural gas, composed predominantly of methane, remains the principal feedstock for commercial hydrogen production owing to its widespread availability and favorable hydrogen-to-carbon (H/C) ratio. In oxidative methane reforming processes, methane is supplied together with oxidizing agents such as H_2O , O_2 , and/or CO_2 , either in the presence or absence of catalysts, to generate synthesis gas (syngas). Because reactions such as steam methane reforming and dry reforming with CO_2 are strongly endothermic, these processes are typically conducted at elevated temperatures ranging from 700 to 1300°C. Furthermore, the water-gas shift reaction is commonly employed to increase hydrogen yield while simultaneously converting carbon monoxide into carbon dioxide [42]. The earliest investigations into plasma-assisted oxidative methane reforming date back to 1897, well before Langmuir formally introduced and defined the term “plasma” [43,44]. Non-oxidative methane (CH_4) conversion is widely regarded as a promising pathway for hydrogen production. Nevertheless, the majority of studies in this field have primarily focused on the generation of higher hydrocarbons as valuable fuels and chemical feedstocks, with hydrogen being produced as a secondary product. Although maximizing hydrogen production is not typically the main objective of non-oxidative CH_4 reforming processes, hydrogen remains an important and valuable product, and these processes could be reconsidered with greater emphasis on enhancing H_2 yields. Direct methane conversion also represents an attractive route for the synthesis of fuels and value-added chemicals. Considerable research efforts have been devoted to advance this area through various approaches, including thermal processing, homogeneous and heterogeneous catalysis, photocatalysis, electrocatalysis, and plasma-catalytic techniques [45].

In parallel with the advancement of innovative hydrogen production technologies, addressing the limitations associated with hydrogen storage remains essential for realizing the full potential of hydrogen as a clean energy carrier. Mortazavi et al. introduced a single-step laser-assisted method for decorating multi-walled carbon nanotubes (MWCNTs) with palladium nanoparticles, thereby modifying the nanotube surface to enhance hydrogen storage performance. Their findings showed that Pd-functionalized MWCNTs exhibit higher hydrogen uptake than untreated MWCNTs. However, the study also revealed the existence of an optimum laser irradiation range, beyond which the storage capacity decreases due to laser-induced structural damage to the material [46]. Mehrabi et al. developed a hybrid approach that combines laser ablation with chemical reduction to decorate multi-walled carbon nanotubes (MWCNTs) with palladium and nickel nanoparticles. This method increases nanoparticle loading on the nanotube surface and generates additional nanocavities, thereby enhancing the effective surface area available for hydrogen adsorption. Characterization techniques, including TEM, XRD, thermal and elemental analyses, BET, and BJH measurements, confirmed the controllability of nanoparticle morphology, distribution, and porosity. Volumetric hydrogen adsorption measurements demonstrated a significant improvement in storage capacity, with maximum hydrogen uptakes of 8.6% and 2.5% for Pd-decorated and Ni-decorated MWCNTs, respectively. The enhanced storage performance was attributed primarily to the hydrogen spillover mechanism and subsequent hydrogen trapping, whereas excessive metal loading resulted in partial pore blockage that adversely affected hydrogen uptake [47]. In a separate study, Mehrabi et al. investigated the influence of nickel nanoparticle decoration on the hydrogen storage performance of MWCNTs using a combined laser ablation and chemical reduction technique. Hydrogen sorption and desorption measurements revealed that hydrogen uptake initially increased with increasing Ni content, reaching an optimum value before declining at higher nanoparticle loadings. The reduction in storage capacity at excessive Ni concentrations was attributed to laser-induced modifications in pore size and pore volume, which decreased hydrogen trapping efficiency, as well as pore blockage and restricted diffusion caused by excessive nanoparticle deposition. The laser-treated samples generally exhibited improved hydrogen trapping characteristics compared to untreated materials. The highest storage capacity was achieved for Ni-decorated MWCNTs containing approximately 12.3–13 wt% Ni, corresponding to hydrogen uptakes of about 1% (or 0.6 wt%, depending on the measurement method). In addition, the Ni-MWCNT samples displayed lower hydrogen desorption temperatures and improved plateau and cycling behavior. The authors also highlighted the economic advantage of Ni over Pd and noted that laser treatment reduced the performance gap between Ni- and Pd-decorated MWCNT systems [48].

This review article offers a broad overview of plasma-assisted hydrogen production methods, with a special focus on discharge-based light and laser techniques such as LIP, SD-LIP, corona discharge, microwave, RF, DBD, and gliding arc systems. It examines the basic mechanisms, reactor designs, performance features, and recent developments in each technology in a critical way. In addition, the comparison between oxidative and non-oxidative plasma methods helps explain why non-oxidative approaches are becoming increasingly preferred for hydrogen production. The article also discusses the main challenges, opportunities, and future directions of plasma-based hydrogen production technologies to support researchers and practitioners in this fast-growing field.

2. Overview of plasma discharge types for hydrogen generation

2.1. Laser-Induced Plasmas

2.1.1. Laser-Induced Plasma (LIP)

The first experimental studies on laser-induced plasma generation appeared shortly after the invention of the ruby laser, with research primarily directed toward understanding fundamental plasma behavior, particle ejection mechanisms, and the underlying processes governing laser–matter interactions [49]. Laser-induced plasma was first observed shortly after the development of the pulsed ruby laser in 1960. One of the earliest published references describing plasma generated by laser irradiation as a spectroscopic source was presented by Brech and Cross in a conference abstract in 1962. Subsequently, the first analytical application of laser-induced breakdown spectroscopy (LIBS) for surface spectrochemical analysis was reported by Debras-Guédon and Liodec in 1963. The systematic advancement of LIBS as an analytical technique gained significant momentum during the late 1970s, largely through research efforts conducted at Los Alamos National Laboratory [50].

Laser-induced plasma (LIP) is commonly considered to be optically thin under Local Thermodynamic Equilibrium (LTE) conditions, implying that collision-driven processes play a much more significant role in determining plasma behavior than radiative interactions [19]. The emission generated from laser-induced plasma is primarily governed by electron-impact excitation processes, whereas photo-excitation mechanisms generally contribute only to a limited extent [51]. The increased population of excited states further enhances the intensity of characteristic emission lines. In addition, the presence of a greater number of initial electrons contributes to the formation of a comparatively larger plasma volume under identical operating conditions [52].

The use of metallic targets can substantially decrease the laser energy required for plasma breakdown, primarily because metals possess higher electron density and greater electron mobility, which facilitate the initiation of the breakdown process [53].

Material ablation commonly accompanies laser-induced plasma formation as a result of both the direct action of the laser beam and the associated thermal effects, particularly those arising from the inverse Bremsstrahlung (IB) heating mechanism. Furthermore, ablation may continue even after the laser pulse has ended, driven by the hydrodynamic forces generated during plasma expansion [20].

When a pulsed laser beam is tightly focused onto a target surface, extremely rapid heating rates exceeding 10^{11} K/s can be achieved, while largely preserving the stoichiometric composition of the generated nanoparticles. The presence of energetic atoms and ions within the laser-induced plasma plume promotes high surface mobility, which plays an important role in nanoparticle formation. During the interaction between the laser pulse and the target material, several mechanisms can lead to the ejection of atoms, clusters, and molten droplets from the surface. Among these mechanisms, pulsed laser ablation is recognized as one of the most widely employed and effective approaches for nanoparticle synthesis [54–56]. This process is based on the condensation of atoms and molecules, followed by cluster formation, with or without accompanying chemical reactions, during the rapid expansion of the vapor or plasma plume generated in front of the target surface. The nucleation

time, as well as the size and composition of the resulting clusters, are strongly influenced by factors such as the target material, laser operating parameters, and the characteristics of the surrounding medium [57].

The electron energy distribution in laser-induced plasma typically spans a range of a few electron volts, allowing multiple electron-impact collisions to induce molecular dissociation and ionization processes. In addition, the presence of metallic catalysts can significantly reduce the effective electron energy required for methane decomposition. However, the electron energy distribution in laser-induced plasma is generally non-Maxwellian and commonly falls within the range of 1–5 eV, whereas methane dissociation requires threshold energies exceeding 9 eV. As a result, methane decomposition through plasma action alone is generally limited, and catalytic assistance plays an important role in enhancing the overall conversion process [58].

The material transferred into the plasma during ablation can exist in several forms, including particles (either freshly generated or molten and subsequently cooled), as well as individual atoms and molecular species. In reality, laser ablation is controlled by a range of complex nonlinear processes. Upon irradiation of the sample surface by the laser beam, material is emitted in the form of electrons, ions, atoms, molecules, clusters, and larger particles, with these ejection mechanisms occurring at different temporal and spatial scales [59,60]. However, under plasma-assisted methane decomposition conditions, the ablated catalyst material predominantly exists in the form of metallic nanoparticles (NPs). These nanoparticles provide active sites for the adsorption of methane molecules, facilitating their catalytic decomposition into intermediate species such as CH_2 radicals, which can subsequently undergo recombination reactions to form higher hydrocarbon compounds [61,62].

The plasma-assisted decomposition of different hydrocarbon molecules has been widely studied and reported in the literature. One of the earliest investigations employing laser-induced plasma generated on the surface of a metallic target to initiate hydrocarbon chemical reactions was published in 1979, marking an important step in the development of laser-plasma-assisted conversion processes [63,64]. In that study, the authors directed a TEA- CO_2 laser beam onto metallic targets, including Pb, Ni, and W, in a methane atmosphere, resulting in the formation of acetylene and molecular hydrogen. Subsequently, the first laser-plasma-assisted heterogeneous catalytic process for methane decomposition was reported using a metal oxide catalyst, specifically Li/MgO, demonstrating the potential of catalyst-assisted laser plasma systems for hydrocarbon conversion [65].

Laser ablation in liquids has emerged as an effective technique for the synthesis of nanoparticles. A distinguishing feature of laser-induced plasma generated in liquid environments is its rapid quenching, which results from the high density of the surrounding medium. When a nanosecond pulsed laser with sufficiently high energy density is focused onto the interface between a liquid and a metallic target, a microplasma layer is produced through a sequence of physical processes. Initially, the laser energy is absorbed by the metal target, leading to the formation of a molten surface layer. Continued energy absorption subsequently raises the local temperature to the metal's boiling point, where several phenomena, including fragmentation, sublimation, and atomization, can occur simultaneously [60,66,67].

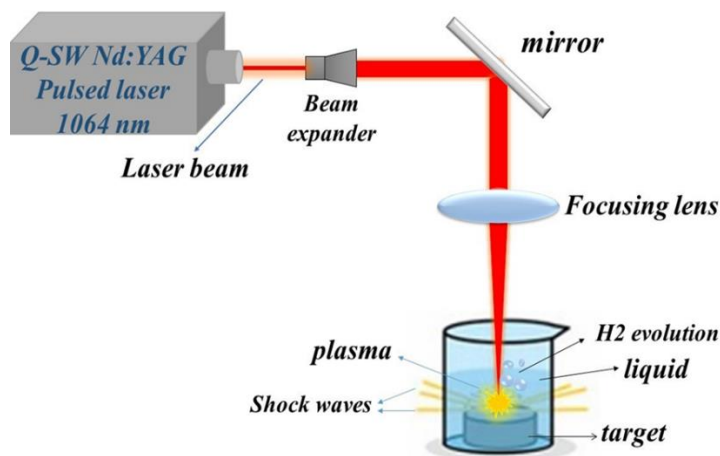


Fig. 1. Schematic of the Laser-Induced Plasma (LIP) setup for hydrogen generation, showing laser focusing on a target in liquid to produce plasma, shock waves, and H₂ evolution.

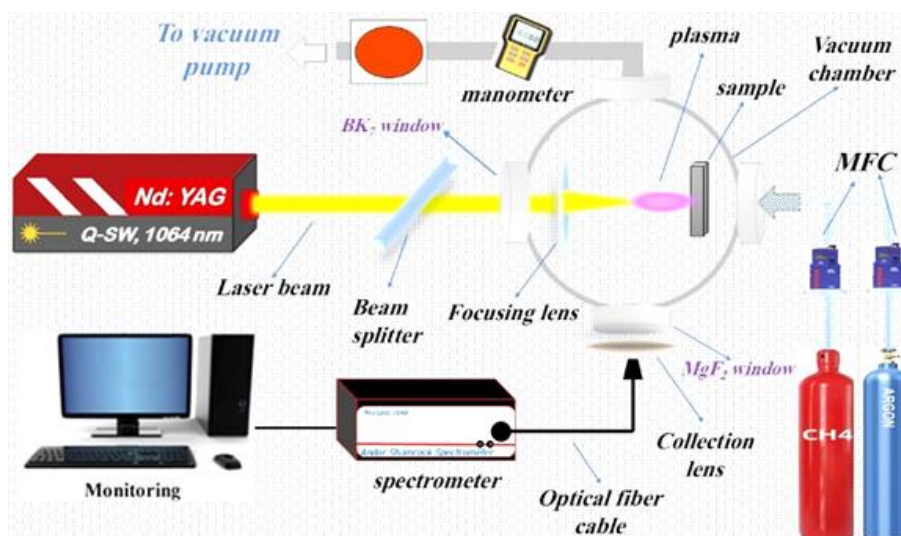


Fig. 2. Laser-induced plasma setup showing laser delivery, focusing optics, vacuum chamber with controlled Ar/CH₄ atmosphere, and plasma emission collection. The system enables precise control of pressure and gas flow for LIP generation and spectroscopic diagnostics.

2.1.2. Spark-Discharge Laser-Induced Plasma (SD-LIP)

Extensive research efforts have been devoted to plasma technologies for improving energy efficiency, including cold plasma systems such as corona discharge (CD) [68,69] and dielectric barrier discharge (DBD) [70,71], as well as warm plasma techniques including gliding arc discharge (GAD) [39,72], spark discharge (SD) [73,74], microwave (MW) plasma [75,76], and radio-frequency (RF) discharge [77]. In general, cold plasma methods are associated with relatively lower conversion efficiencies, whereas warm plasma systems provide higher gas temperatures, elevated electron densities, and greater electron energies, thereby promoting more effective decomposition processes. However, excessive heating can also accelerate coke

formation, which inhibits key reaction pathways and ultimately reduces or even terminates methane conversion performance [78].

Furthermore, the sophisticated power supply systems required for hot plasma technologies, particularly radio-frequency (RF) and microwave (MW) discharges, significantly increase equipment costs and can limit the economic feasibility of large-scale implementation. Consequently, spark discharge has emerged as an attractive option among warm plasma techniques, especially when integrated directly with solid catalysts. In practice, the pulsed nature of spark discharges helps mitigate excessive heating, as the intervals between successive discharge events provide cooling periods that reduce overheating and improve process stability compared with continuously operated plasma systems [74,79,80].

In spark discharge (SD) systems, the conventional configuration generally comprises two electrodes connected to a charged capacitor, which serves as the energy source for generating the discharge plasma [81]. When a sufficiently high voltage (V_0) is applied across the electrodes, the discharge process begins with the formation of a streamer. As the streamer propagates and reaches the opposing electrode, electrical breakdown occurs, resulting in the transition of the streamer into an expanding plasma channel. Within this plasma column, Joule heating raises the temperature of both the plasma and the electrode surfaces. Simultaneously, energetic ions bombard the electrodes, causing sputtering of electrode material, a process that bears similarities to laser ablation. In the presence of a background gas, the sputtered species rapidly thermalize and nucleate to form primary nanoparticles, which can subsequently grow through collisions, leading to the formation of larger particles or aggregates.

In spark discharge systems, a reduction in gas density lowers the plasma resistivity, thereby limiting additional energy transfer from the electric current into the plasma. As the plasma expands, it cools while the surrounding gas flows back toward the discharge axis. These processes can repeat cyclically when the absorbed energy is sufficient to sustain further plasma expansion, resulting in periodic discharge behavior [82]. When a streamer successfully bridges the gap between two electrodes, and neither a pulsed power supply nor a dielectric barrier is present (as in corona discharge and DBD systems, respectively), the discharge current can continue to increase, leading to the formation and development of a spark discharge [83]. It should be noted that, according to Paschen's law, the breakdown voltage required for spark discharge initiation depends strongly on both the gas pressure and the distance separating the electrodes [84]. In contrast, the incorporation of a laser can substantially lower the breakdown voltage relative to a standalone spark discharge system. This effect is primarily attributed to inverse bremsstrahlung heating, which increases the electron density within the discharge region and thereby facilitates electrical breakdown [16]. As a result, spark discharges can be generated across electrode gaps as large as 6 mm while operating at lower applied voltages. This feature is particularly important because it considerably reduces electrode erosion and corrosion, which remain among the primary limitations affecting the long-term operation of industrial plasma systems [12].

Fortunately, the SD-LIP configuration benefits from the synergistic interaction between spark discharge and laser-induced plasma, which significantly strengthens the local electric field and increases both the mean electron energy and electron density through the inverse Bremsstrahlung mechanism. The resulting plasma environment enhances collision frequencies between electrons and methane molecules, thereby improving energy conversion efficiency (ECE) processes and hydrogen production while reducing undesirable energy loss channels. Although a conventional spark discharge may generate a higher

overall thermal load than the SD-LIP system, it generally produces a lower electron density. Experimental observations indicate that SD-LIP generates a considerably denser electron population than spark discharge alone, making it more effective for promoting recombination reactions. Consequently, recombination rates are enhanced in the SD-LIP system, even though the plasma temperature remains lower than that observed in the SD mode. In practice, a larger fraction of the supplied energy is utilized for methane conversion rather than being dissipated as heat, contributing to the improved efficiency of the SD-LIP process [16].

In spark-assisted LIBS (SA-LIBS), the application of an electrical discharge enhances the relative signal intensity ratio by reheating the laser-induced plasma and prolonging its lifetime, thereby improving the overall spectroscopic signal quality [85]. In addition, various spark discharge configurations employing customized electrical circuits and different electrode geometries have been developed and applied to meet specific operational and experimental requirements [86–88].

The accumulation of substantial coke deposits and the resulting coverage of active catalytic sites can cause rapid catalyst deactivation. Therefore, identifying operating conditions that provide an appropriate balance between energy efficiency, reactant conversion, and coke suppression remains one of the major challenges in non-oxidative methane conversion processes. Based on our findings, the integrated use of a solid catalyst and spark discharge in conjunction with laser-induced plasma treatment can effectively suppress coke formation and help maintain catalyst activity over extended operation periods [16]. It is important to note that the hybrid SD-LIP system enables efficient cleaning of the catalyst surface after each laser pulse by ablating accumulated carbon soot (coke), thereby slowing catalyst deactivation. Thus, the laser plays a dual synergistic role by facilitating both controlled discharge ignition and continuous coke removal. In addition, the electrical spark discharge contributes significantly to the overall system power and offers a more accessible and cost-effective approach for methane decomposition compared with laser-induced plasma alone in terms of energy consumption. Consequently, the integration of laser-induced plasma with spark discharge not only improves process efficiency but also greatly enhances operational controllability. Such characteristics are particularly advantageous in applications where high reliability and superior performance are required, including onboard transportation systems and compact petrochemical processing units [18].

The Laser-Triggered Spark Discharge (LTSD) technique integrates the operational simplicity and pulsed-power advantages of spark discharge with the precision, electron-density enhancement, and self-cleaning capabilities of laser-induced plasma. Through this synergistic combination, LTSD can effectively address several limitations associated with conventional spark discharge systems, including poor energy efficiency, catalyst coking, and performance degradation at elevated pressures. As a result, it provides a more selective, efficient, and reliable platform for hydrogen production from hydrocarbon feedstocks such as propane. It is worth noting that many conventional hydrocarbon conversion methods generate substantial amounts of carbon dioxide alongside hydrogen. In contrast, the LTSD approach enables the non-oxidative conversion of propane, allowing hydrogen to be produced directly without significant CO₂ formation. Consequently, this technology offers a promising route for transforming hydrocarbon gases into clean hydrogen fuel while minimizing greenhouse gas emissions. Such decarbonized hydrogen production pathways are of considerable importance for environmental protection and the long-term sustainability of future energy systems.

In the LTSD process, energy conversion efficiency can be substantially improved by increasing key operating parameters such as spark voltage, laser pulse energy, and the number of laser shots. In addition to these factors, reactor volume plays a critical role in determining the overall conversion performance and should be taken into account when evaluating and comparing different reactor configurations and processing systems.

Despite its distinctive advantages, the LTSD technique still presents several potential limitations. First, the requirement for a laser system increases the overall capital cost of the process; however, continuous technological advancements have considerably reduced the cost of laser equipment over the past decade, improving its practical feasibility. Second, further improvements in process efficiency are still needed to enhance the attractiveness of the technology for industrial-scale deployment. This limitation may be addressed through the use of optimized hybrid catalyst systems, higher-intensity laser irradiation, and more effective spark discharge conditions, particularly in large-scale applications where improved conversion performance can be achieved [17].

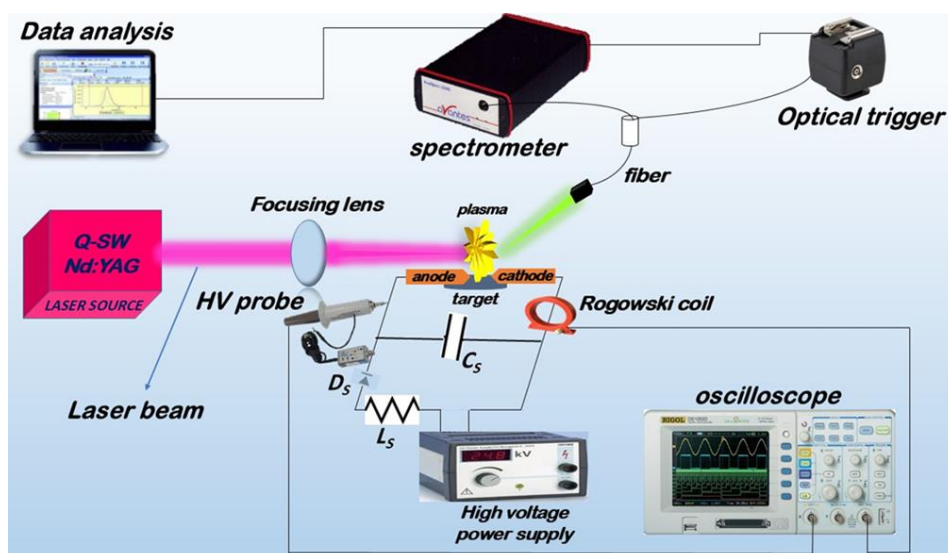


Fig. 3. Experimental configuration of the SD-LIP technique, highlighting the optical path and the integrated diagnostic tools (spectrometer, Rogowski coil, and oscilloscope) used for characterizing the ablation process.

2.2. Electrical Discharge Plasmas

2.2.1. Dielectric Barrier Discharge (DBD)

Dielectric barrier discharge (DBD) plasma is among the most widely utilized techniques for generating non-thermal plasma in research and laboratory applications. Its extensive adoption can be attributed to several practical advantages, including simple reactor design and operation, the ability to function under ambient conditions, and the flexibility to perform repeated start-up and shutdown cycles with minimal operational complexity [89–91]. Dielectric barrier discharge (DBD) reactors are typically composed of two electrodes connected to a power supply, with one or more insulating dielectric layers positioned between the electrodes to regulate the discharge behavior and prevent the formation of continuous arcs [91–93]. In most cases, DBD plasmas are generated using either planar electrode arrangements or coaxial reactor configurations, both of which are commonly employed depending on the specific application and reactor design requirements [91]. The dielectric barrier

typically has a thickness of a few millimeters and is commonly fabricated from materials such as quartz, glass, ceramics, or various polymeric compounds, depending on the operating conditions and reactor design [94]. The thickness of the electrodes is generally in the range of several tens of micrometers [95], whereas the discharge gap may range from a few millimeters to several centimeters, depending on the specific reactor configuration and intended application [96]. When a sufficiently high voltage is applied across the electrodes, the gas occupying the discharge gap undergoes electrical breakdown and forms a plasma. The presence of the dielectric barrier limits the discharge current and suppresses the transition to a continuous arc or spark discharge, thereby maintaining stable non-thermal plasma operation [97,98]. As a result, DBD plasmas are frequently described as silent discharges because the dielectric barrier prevents complete gas breakdown and inhibits the formation of a continuous arc within the discharge region [89]. The self-limiting behavior of DBD plasma results in the generation of short-lived filamentary microdischarges, typically exhibiting extinction times on the order of 10^{-7} s. These filaments are characterized by very high localized electron densities, which can reach values as high as 10^{15} cm⁻³, while maintaining non-thermal plasma conditions throughout the discharge process [98].

In addition, the discharge characteristics of DBD plasmas are strongly influenced by operating parameters such as applied voltage, excitation frequency, gas composition, and temperature. Depending on these conditions, the plasma may exhibit either filamentary behavior or a more homogeneous diffuse discharge mode [96]. DBD plasma systems are generally operated under atmospheric-pressure conditions and at relatively low gas temperatures. In most experimental configurations, the plasma is driven by an alternating current (AC) power supply, typically functioning within the kilohertz (kHz) frequency range [92,94]. In more contemporary research, there has been a transition toward utilizing radio frequency or pulsed plasma systems that operate within the megahertz (MHz) frequency spectrum [92]. Operating within these elevated frequency ranges leads to a reduction in the voltage required for gas breakdown [99]. Furthermore, instead of accumulating on the dielectric material, the charges are maintained within the discharge gap [92]. Due to these characteristics, Dielectric Barrier Discharge (DBD) plasma has become the primary choice for numerous investigations into plasma-catalysis [100].

Within a DBD reactor setup, an elevation in discharge power typically results in a higher density of micro-discharge filaments, which subsequently provides more numerous channels for chemical reactions to occur [101,102]. The discharge power in a DBD system is largely governed by the number of streamer discharges generated per unit area and per unit time. For air-based DBD plasmas, a typical streamer density is on the order of 10^6 cm⁻² s⁻¹, reflecting the high frequency of microdischarge events occurring within the plasma volume [103].

Dielectric Barrier Discharge (DBD) has established itself as the most prevalent plasma configuration, specifically for applications involving partial oxidation (POX) and dry reforming of methane (DRM) [104]. The prominence of DBD systems is attributed to several key benefits, including their low-temperature operation, compact architecture, and structural simplicity, alongside their versatility in handling diverse feedstocks and the ease with which catalysts can be integrated. The effectiveness of plasma-assisted oxidative methane reforming is directly influenced by the electrode configuration [105], the dielectric properties of the packing materials [106–109], and the specific geometries of the reactor and dielectric barrier [110–113]. Typically, DBD-driven hydrogen production processes exhibit an energy efficiency of approximately 6–10%, achieving H₂ yields in the range of 30–40%. In an investigation of DBD plasma-assisted dry reforming of methane (DRM), Li et al. [105] demonstrated that titanium (Ti) electrodes achieve superior methane conversion rates compared to those made of

aluminum (Al), iron (Fe), or copper (Cu). Khoja et al. [104] evaluated a cylindrical DBD reactor by varying the discharge gap from 1 to 5 mm and the discharge length from 100 to 300 mm, concluding that the most effective performance was achieved with a 3 mm gap and a 300 mm length. Wang and colleagues [104,110] engineered a multistage DBD reactor configuration characterized by a series of ground electrodes arranged in tandem, all of which operated in conjunction with a single shared high-voltage electrode. The study revealed that the multistage DBD configuration enhanced hydrogen selectivity relative to traditional single-stage designs. This improvement was attributed to the integration of quenching zones between the ground electrodes, which effectively suppressed the recombination of CO_2 and thereby favored the desired product distribution [110].

Furthermore, existing research indicates that integrating a DBD system with a catalyst—a configuration known as plasma catalysis—enables the fine-tuning of process selectivity toward the intended chemical products [114–116].

From a practical standpoint, DBD systems offer distinct advantages over alternative plasma sources, such as microwave and gliding arc discharges, due to their structural simplicity, mechanical robustness, and inherent scalability. The industrial feasibility of this technology was established over 150 years ago through its successful commercial implementation for ozone production [83,117].

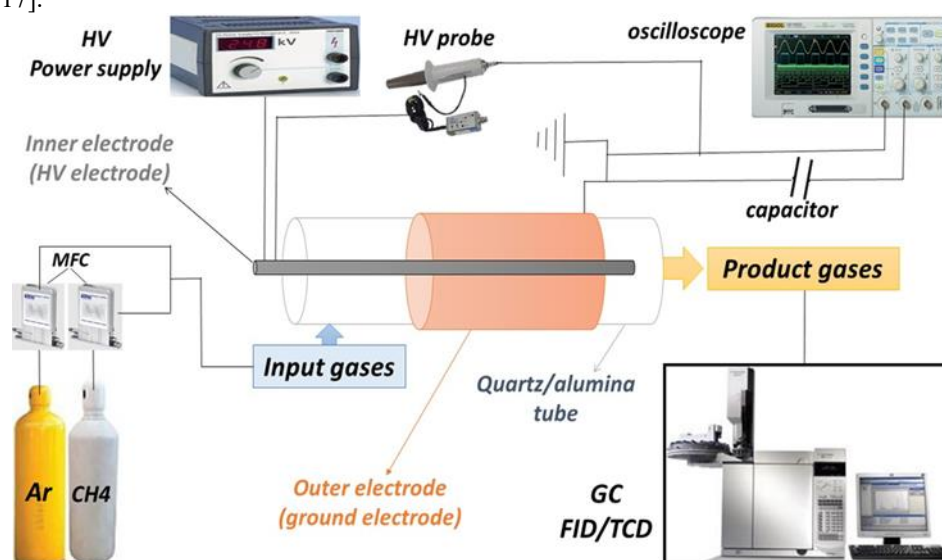


Fig. 4. Schematic diagram of a dielectric barrier discharge (DBD) reactor for hydrogen production via methane reforming, showing the coaxial quartz/alumina discharge tube, high-voltage and grounded electrodes, Ar/CH₄ gas supply system, gas chromatography product analysis, and electrical diagnostics.

2.2.2. Corona Discharge

Corona discharge derives its name from its characteristic appearance, which resembles a luminous crown surrounding the electrode [23]. It is generally classified as a low-power electrical discharge and is typically non-uniform in nature. Corona discharges are characterized by the presence of a strong electric field, relatively low current density, and intense localized light emission concentrated in the vicinity of one of the electrodes [118]. This partial self-sustained gas discharge can be generated in a sufficiently strong and non-uniform electric field under atmospheric-pressure conditions, using either alternating current (AC) power supplies or continuous/pulsed direct current (DC) sources. Various electrode arrangements

have been employed in corona discharge systems. One of the most common configurations consists of a grounded outer plate electrode combined with a concentric high-voltage wire or rod serving as the inner electrode, as illustrated in **Fig. 5** [119]. Alternatively, corona discharge reactors may employ point-to-point or point-to-cylinder electrode arrangements. The use of asymmetric electrode geometries is particularly effective in enhancing discharge stability, although it generally results in a smaller plasma volume. In most cases, corona discharges are generated in regions where the electric field strength is highly concentrated, such as near sharp tips, edges, or thin wires with small radii of curvature. The discharge formation mechanism is strongly influenced by electrode polarity, giving rise to different discharge modes, including positive corona, negative corona, bipolar corona, alternating-current (AC) corona, and high-frequency (HF) corona. While DC and pulsed-DC systems can be operated with either positive or negative polarity, AC-powered reactors do not exhibit persistent polarity-dependent effects.

A positive corona is formed when the strongest electric field is concentrated around the anode. Under sufficiently high voltages, this discharge mode can more readily evolve into a spark discharge. In contrast, a negative corona develops when the high-field region is localized around the cathode and is generally characterized by greater discharge stability, although it operates over a more limited voltage range [23]. Compared with plasma-assisted steam methane reforming (SMR) and partial oxidation (POX) processes, corona discharge systems have been more frequently applied to dry reforming of methane (DRM). These systems typically exhibit an energy efficiency of approximately 10.7% and can achieve hydrogen yields of around 56%. Previous studies have shown that positive corona discharges generally provide higher reactant conversion in plasma-assisted DRM than negative corona discharges. This improvement is mainly attributed to the larger active plasma volume and the higher electron energies associated with positive corona operation. Nevertheless, negative corona discharges offer certain advantages for hydrogen production, as they can enhance the H₂ yield and facilitate the attainment of H₂/CO ratios that exceed those obtained under positive corona conditions [120]. Li et al. similarly reported that methane conversion in various corona discharge modes followed the sequence positive corona > AC corona > negative corona. Using a positive corona discharge for the dry reforming of methane (DRM) process at a specific energy input (SEI) of 45 kJ/L, they achieved methane conversion and hydrogen yield values of approximately 70%, together with an energy efficiency of 14.3%. Interestingly, the influence of discharge mode on the syngas composition exhibited an opposite trend, with the H₂/CO ratio following the order negative corona > AC corona > positive corona. This observation indicates that although positive corona discharges are generally more effective for methane conversion and hydrogen generation, negative corona discharges may be preferable when a higher H₂/CO ratio is desired in the final syngas product [121].

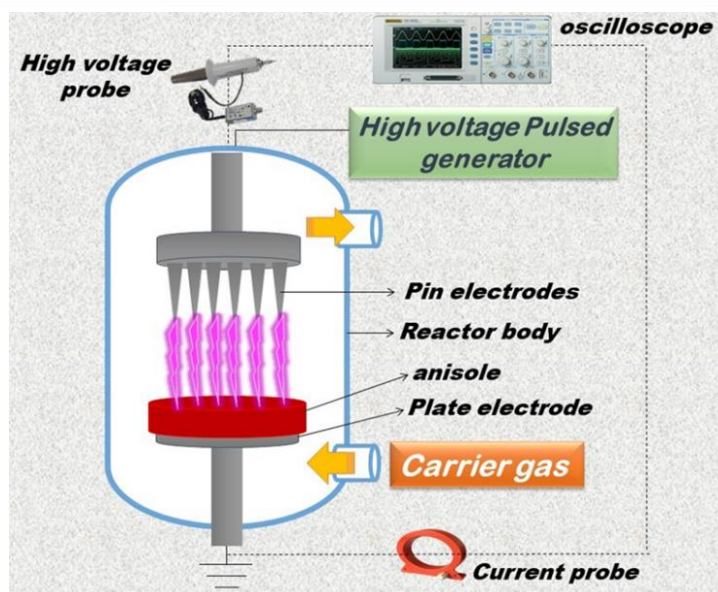


Fig. 5. Schematic representation of a point-to-plane pulsed corona discharge reactor. Adapted from Ref. [119].

2.2.3. Gliding Arc / Rotating Gliding Arc (GA/RGA)

Gliding arc (GA) discharges represent one of the most widely employed types of warm plasma and are characterized by higher bulk gas temperatures and current densities than those observed in corona discharge or dielectric barrier discharge (DBD) systems. Owing to these characteristics, GA discharges generally offer superior energy efficiency and an enhanced capacity for treating large gas volumes. The most commonly utilized GA configuration is the quasi-two-dimensional reactor, which consists of two or more diverging metallic electrodes, as illustrated in **Fig. 6(a)** [122]. In typical gliding arc systems, torch-like plasma arcs are generated between knife-shaped electrodes energized by either DC or AC power supplies. Arc ignition initially occurs at the smallest gap between two flat, diverging electrodes, where the electric field strength is greatest. Subsequently, the gas flow transports the arc toward regions with larger electrode separation distances. As the plasma column elongates and expands, the gas temperature decreases rapidly, whereas the electron temperature remains relatively high. Consequently, the discharge undergoes a rapid transition from thermal to non-thermal ionization, occurring on a nanosecond timescale. This non-thermal ionization process accounts for approximately 75–80% of the total discharge energy, contributing significantly to the efficiency of gliding arc plasmas [123–125]. As the distance between the electrodes continues to increase, the arc eventually extinguishes, after which a new discharge is reignited at the location corresponding to the minimum interelectrode gap. This cyclic process repeats continuously during reactor operation. Therefore, relatively high gas flow rates are required to sustain arc propagation and ensure stable discharge behavior in gliding arc systems. Despite their advantages, conventional GA reactors face several important challenges, including limited reactant conversion resulting from the short residence time of the gas within the active plasma region and electrode degradation caused by carbon deposition and fouling on the electrode surfaces [126–127]. To overcome these limitations, several studies have proposed the use of rotating gliding arc (RGA) systems, which offer improved plasma stability, enhanced gas–plasma interaction, and reduced electrode fouling compared with conventional gliding arc reactors [4]. Recent research has focused on advancing rotating gliding arc (RGA)

reactor designs to enhance the residence time of reactants within the plasma zone and thereby improve conversion performance. Zhu and co-workers developed an innovative RGA reactor driven simultaneously by a tangential gas flow and an external magnetic field. Through the combined action of the swirling gas motion and the Lorentz force, the arc was able to rotate rapidly and stably around a cone-shaped inner electrode, generating a large and stable three-dimensional plasma region while significantly increasing reactant residence time. Using a downstream-packed 10 wt% Ni/ γ -Al₂O₃ catalyst, the system achieved a methane conversion of 58.5% and a hydrogen yield of 20.7%, demonstrating the effectiveness of this reactor configuration for plasma-assisted methane conversion [128]. In addition, Lu et al. investigated the influence of electrode geometry on the dry reforming of methane (DRM) in a rotating gliding arc reactor with spiral gas feeding (**Fig. 6.b**). Parameters such as the summit angle of the inner electrode and the length of the outer electrode were systematically evaluated. Their results showed that an inner electrode summit angle of 45° produced the highest methane conversion (28%) and hydrogen yield (16%). This performance was attributed to an optimal balance between the available arc-sliding distance and the arc rotation time near the electrode tip. The study also demonstrated that increasing the length of the external electrode promoted greater arc extension, resulting in a 27% improvement in methane conversion compared with configurations employing a shorter external electrode [129]. Furthermore, in addition to optimizing electrode geometries, other reactor design modifications have also been explored, including the incorporation of a three-dimensional nozzle [130] and a water-cooled quenching rod [131]. These engineering improvements have been shown to enhance hydrogen production performance while simultaneously increasing the overall energy efficiency of the plasma conversion process. The former study attributed the observed improvements to a reduction in heat losses resulting from flow-induced thermal insulation within the reactor [130]. In contrast, the latter study emphasized that the incorporation of a quenching device effectively suppressed the reverse water–gas shift (RWGS) reaction, a side reaction that consumes hydrogen, thereby contributing to enhanced hydrogen production and overall process efficiency [131]. Compared with other non-thermal plasma reforming technologies, gliding arc systems can operate at relatively low specific power consumption while maintaining effective reactant conversion. As a result, they are capable of achieving comparatively high energy efficiencies, making them attractive for plasma-assisted reforming applications [132].

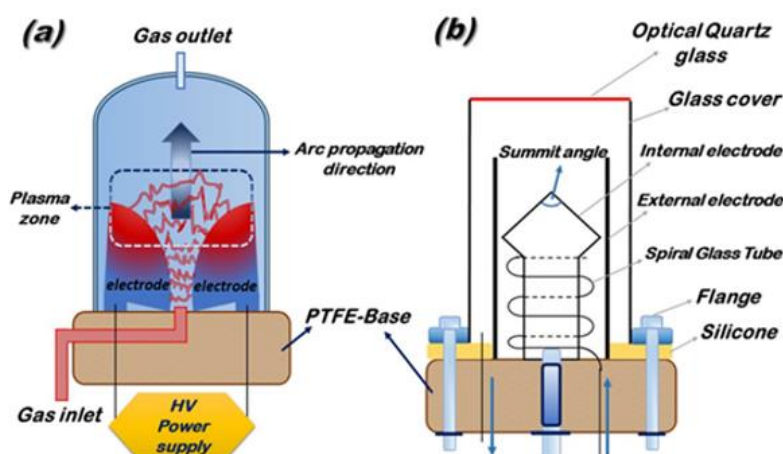


Fig. 6. Schematic diagrams of (a) a gliding arc (GA) reactor and (b) a rotating gliding arc (RGA) reactor for hydrogen production, illustrating the electrode configuration, arc propagation, gas flow path, and plasma region. Adapted from Refs. [122,129].

2.3. Electromagnetic Field-Driven Plasmas

2.3.1. Microwave (MW) Plasma

Microwave (MW) plasma is generally classified as a warm plasma and exhibits several characteristics that are comparable to those of thermal plasmas. Owing to the high operating frequencies employed in MW systems, typically ranging from 300 MHz to 10 GHz, energy transfer and dissipation within the plasma are significantly greater than those observed in many other plasma reactor configurations [133]. Microwave (MW) discharges offer several important advantages, including high reactant conversion, favorable product selectivity, and the capability to process large gas volumes. Moreover, microwave plasma generation is an electrode-free process, which minimizes contamination and eliminates electrode-induced side reactions, thereby producing a relatively pure plasma environment. A schematic representation of a typical microwave plasma system is presented in **Fig. 7** [134]. Microwave discharge systems typically operate at frequencies of either 2.45 GHz or 915 MHz and consist of several key components, including a magnetron source, a circulator, a stub tuner, a waveguide, a plasma discharge tube, and a post-discharge chamber. Together, these components ensure efficient microwave power delivery, plasma generation, and subsequent processing of the reaction products [134,135]. In such systems, microwave radiation is generated by a magnetron and subsequently transmitted to the reaction chamber through a waveguide. A dielectric tube, typically fabricated from quartz because of its excellent transparency to microwave radiation, is positioned within the waveguide. When the process gas flowing through the dielectric tube passes through the microwave field region, free electrons within the gas absorb microwave energy, initiating ionization processes and leading to plasma formation [136]. Microwave power can be concentrated within a localized region at the intersection of the waveguide and the dielectric tube, where efficient energy coupling leads to the generation of microwave plasma. The resulting plasma is characterized by a high ion density, typically exceeding 10^{11} cm^{-3} . Moreover, the bulk gas temperature can vary over a wide range, from near ambient conditions to several thousand kelvin, depending on the applied microwave power and operating conditions [137]. Microwave plasma can be generated in several distinct discharge modes, including surface-wave discharges, electron cyclotron resonance (ECR) discharges, cavity-induced discharges, and freely expanding atmospheric-pressure plasma torches. Each configuration offers unique plasma characteristics and operational advantages depending on the intended application and processing requirements [138]. Despite their numerous advantages, microwave plasma systems generally require relatively complex equipment and power-delivery components, which can significantly increase the overall capital and operational costs of the technology [139].

Microwave (MW) discharges have demonstrated excellent performance in hydrogen production processes, offering high reactant conversion, high hydrogen selectivity, and the capability to treat large gas volumes. Reported hydrogen yields typically range from 50% to 100%, depending on the operating conditions and feed composition. As an electrode-free technology, MW plasma systems effectively eliminate problems associated with electrode contamination, erosion, and soot accumulation. Furthermore, the energy efficiency of microwave plasmas for hydrogen production, generally reported in the range of 24–47%, is comparable to that achieved by atmospheric-pressure plasma jets, spark discharges, and atmospheric-pressure glow discharges. Consequently, numerous studies have emphasized the significant potential of atmospheric-pressure microwave plasma as an effective technology for hydrogen generation [30,31,140,141].

Early investigations into microwave plasma technology proposed the use of microwave-induced liquid plasma for the decomposition of methane hydrates in subsea environments as a potential route for hydrogen production. This approach was considered particularly attractive because of the vast reserves of methane hydrates available in marine sediments and the possibility of converting them directly into hydrogen at the extraction site [142]. More recently, Wang et al. advanced this concept by developing an innovative microwave liquid-discharge system for plasma-assisted steam methane reforming (SMR). In this approach, the reforming reaction occurs directly within liquid water, thereby minimizing discharge instabilities commonly associated with carbon deposition. The technology provides a practical alternative for processing multiphase mixtures of gaseous methane and liquid water, eliminating the need for prior water vaporization and simplifying the overall reforming process while maintaining effective hydrogen production performance [143].

The principal advantages of microwave discharges include their ability to ignite plasma readily, operate over a wide range of pressures, process large volumes of gas efficiently, and avoid contamination of the reaction medium by electrode erosion products due to their electrode-free nature. These characteristics make microwave plasma systems highly attractive for a variety of plasma-assisted chemical conversion and hydrogen production applications [144].

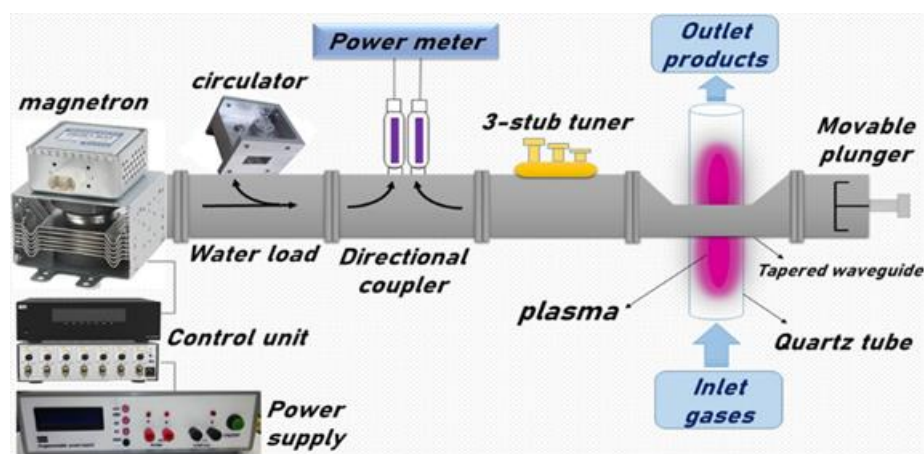


Fig. 7. Representation of a microwave plasma setup for hydrogen production, showing waveguide-based power delivery to sustain plasma within a quartz tube reactor, enabling gas inlet and product outlet for reforming processes.

2.3.2. Radio Frequency (RF) Plasma

As early as 1956, the Soviet physicist Vladimir Veksler proposed that the force exerted by a radio-frequency (RF) electromagnetic field on a plasma could be sufficiently strong to influence its behavior significantly. He suggested that an appropriately designed RF field configuration might simultaneously confine and accelerate a plasma. One year later, Knox independently proposed the use of RF fields generated within a spherical resonant cavity to confine a thermonuclear plasma. These pioneering ideas stimulated considerable theoretical research during the subsequent years, leading physicists in the Soviet Union, Britain, and the United States to investigate RF-based plasma confinement and control in greater detail [145]. An RF plasma torch typically consists of an induction coil surrounding an insulating tube through which the process gas flows. The alternating current passing through the induction coil generates an oscillating magnetic field that induces eddy currents within the plasma, resulting in heating through the Joule effect. One of the principal advantages of RF plasma torches is their electrode-free design, which eliminates problems associated with electrode erosion, degradation, and corrosion during

operation. However, compared with conventional DC plasma torches, RF plasma torches generally produce lower plasma jet velocities and achieve maximum temperatures of approximately 10,000 K [146]. Radio-frequency (RF) discharges typically operate within the frequency range of 1–100 MHz, corresponding to wavelengths of approximately 300–3 m, which are considerably larger than the dimensions of most plasma reactors. Power can be coupled into the plasma either capacitively or inductively, leading to two principal configurations: capacitively coupled plasma (CCP) and inductively coupled plasma (ICP). Owing to their stable operation and controllable plasma characteristics, these discharge systems are widely employed in applications such as thin-film deposition, plasma etching, material sputtering, and as ion sources in mass spectrometry [147]. Radio-frequency (RF) power is delivered to plasma reactors through either inductive or capacitive coupling configurations, as illustrated in **Figs. 8(a)** and **8(b)**. A key component of these systems is the impedance matching unit (matching box), which is installed between the external RF power generator and the plasma reactor. The matching network ensures efficient power transfer, minimizes reflected power losses, and contributes to stable and reliable plasma operation under varying process conditions [148].

Longmier et al. investigated hydrogen production from methane using a 13.56 MHz RF helicon plasma reactor operating under total non-ambipolar flow conditions. The high-density non-thermal plasma, with electron densities exceeding 10^{13} cm^{-3} , enabled extensive methane dissociation, while ion confinement and recirculation within the reactor increased the likelihood of repeated ionization and decomposition events. Under operating conditions of 1300 W RF power and a methane flow rate of 8 SCCM, the reactor achieved a methane conversion efficiency of $99.99 \pm 0.06\%$, yielding high-purity hydrogen and solid graphite as the primary products. Although the overall energy efficiency remained lower than that of conventional steam methane reforming, the process offered the important environmental advantage of producing solid carbon rather than carbon dioxide, highlighting the potential of RF helicon plasma technology as a cleaner pathway for hydrogen generation from methane [149].

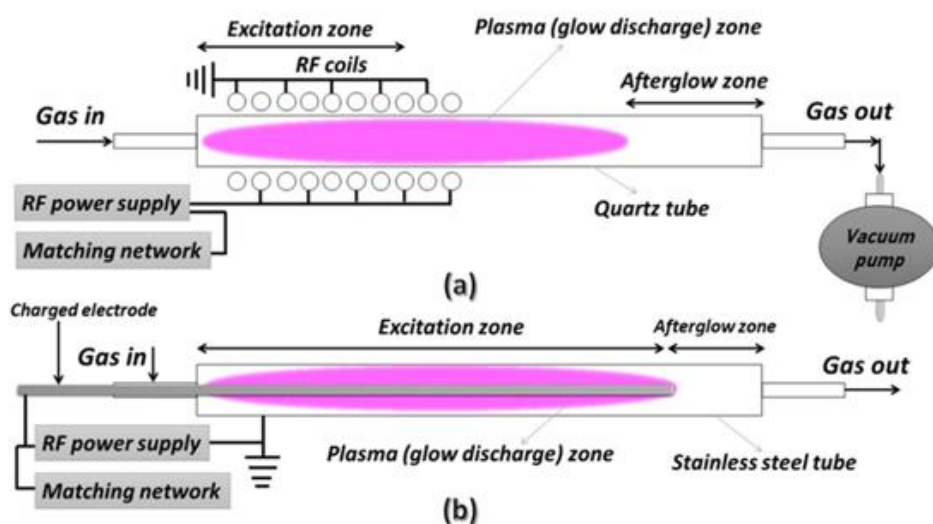


Fig. 8. Schematic diagrams of radio-frequency (RF) plasma systems for hydrogen production: (a) inductively coupled plasma (ICP) and (b) capacitively coupled plasma (CCP) configurations. Adapted from Ref. [148].

Radio-frequency (RF) plasma irradiation can be readily employed to generate stable plasmas in water, even under high-pressure conditions [150]. Moreover, studies have reported that the energy required for the production of hydrogen, oxygen, and hydrogen peroxide from water at atmospheric pressure represents only a small fraction of the applied RF power, corresponding to approximately 0.4% of a 150 W RF power input [33]. These findings demonstrate the feasibility of RF plasma technology for liquid-phase plasma generation and water-based chemical conversion processes.

3. Plasma-Catalytic Synergy and Mechanisms

Deciphering the fundamental mechanisms and the relative contributions of the plasma, the catalyst, and their synergistic interplay remains the most formidable challenge in the field. The interactions between plasma and catalysts induce diverse phenomena, such as local electric field intensification, modifications to the discharge mode, and the development of micro-discharges within the catalyst pores. This multi-faceted interaction introduces a high degree of complexity, which complicates the systematic design and optimization of these processes [4]. The interactions between plasma and catalysts are profoundly complex, characterized by a reciprocal influence where the catalytic material alters the plasma's behavior while the plasma simultaneously modifies the physicochemical properties of the catalyst [151]. In one aspect, the integration of packing media significantly modulates the characteristics of the plasma discharge. This includes the initiation of micro-discharges within pores that exceed the Debye length, the propagation of streamers across catalyst surfaces, and fluctuations in the discharge volume, alongside localized electric field intensification. These phenomena directly influence the electron energy distribution and the frequency of electron-impact collisions, which ultimately drives shifts in the distribution and yield of chemical species within the plasma phase [152]. Conversely, plasma exposure can enhance the intrinsic properties of a catalyst, including its surface area, redox state, defect density, and electron extraction potential [153–157]. Furthermore, the initiation of micro-discharges in proximity to regions of high surface curvature can lead to the formation of localized 'hot spots' on the catalytic material [158]. Crucially, the presence of reactive species—such as free radicals and vibrationally excited molecules—can effectively lower the activation energy required for surface-mediated reactions, thereby establishing alternative kinetic pathways that facilitate the formation of target chemical products [152]. The cooperative interplay between plasma and integrated catalysts can overcome many of the inherent limitations of standalone plasma processes, such as suboptimal hydrogen selectivity. For instance, the use of zeolites [159–163], γ - Al_2O_3 [164], and Ni- or Mn-based catalysts [35] promotes hydrogen generation via plasma-mediated surface reactions. This exceptional synergy has fostered the development of innovative and highly efficient strategies for hydrogen production [4]. Moreover, adsorption-desorption dynamics at the catalyst interface lead to a substantial elevation in H radical density and H_2 consumption rates in the immediate vicinity of the surface. This research underscores that the catalyst plays a critical role in reshaping the spatial profiles of reactive intermediates, thereby indirectly steering the broader plasma-phase chemical pathways [165].

Dielectric Barrier Discharge (DBD) has emerged as the most widely implemented plasma source across a broad range of plasma-catalytic investigations [100]. The integration of DBD plasma with catalytic materials is typically achieved through two primary configurations: (I) in-plasma catalysis (IPC), also known as single-stage catalysis, where the catalyst is positioned directly within the discharge zone; and (II) post-plasma catalysis (PPC), or two-stage catalysis, where the catalytic bed is situated downstream of the plasma source. In PPC systems, the catalytic interactions are primarily limited to long-

lived plasma species or stable intermediates. Conversely, the IPC configuration allows for the interaction of short-lived, high-energy entities—such as ions, radicals, and electronically or vibrationally excited molecules—with the catalyst surface, thereby facilitating novel pathways for chemical conversion [166]. To enhance methane activation and hydrogen selectivity, Indarto explored the use of zinc and chromium oxide catalysts within a DBD reactor. The findings demonstrated a notable improvement, with methane conversion reaching approximately 50% in the plasma-catalytic system compared to the non-catalytic baseline, while the presence of the catalyst simultaneously boosted hydrogen selectivity to 40% [167]. While quantitative data regarding carbon deposition was not provided in the study, the accumulation of carbonaceous species was observed on the reactor walls and inner electrode surfaces, ultimately resulting in the deactivation of both the catalyst and the reactor.

Khalifeh et al. investigated methane decomposition for hydrogen generation using a nanosecond pulsed DBD reactor across three distinct configurations: a plasma-only baseline, a packed-bed system (utilizing glass beads), and a plasma-catalytic setup (employing Pt-Re/Al₂O₃). Their findings indicated that at lower methane flow rates—specifically 20 mL/min, corresponding to a residence time of 9.46 s—the conversion efficiency followed the sequence: plasma with packing > plasma with catalyst > standalone plasma. Conversely, as the flow rate was increased to 30 mL/min (residence time of 8.28 s), the plasma-catalytic system became dominant, exhibiting the highest methane conversion in the order of: plasma with catalyst > plasma with packing > standalone plasma. It was noted that further elevating the flow rate to 40 mL/min (7.36 s) destabilized the discharge, resulting in a total loss of conversion. Regarding hydrogen productivity, the packed-bed configuration reached a peak rate of 0.891 mmol/min at a 20 mL/min flow rate; however, at 30 mL/min, the catalytic plasma system surpassed it, achieving a maximum hydrogen production rate of 1.213 mmol/min [168].

Li et al. investigated a two-stage plasma-catalytic system utilizing a Ni-modified H-ZSM-5 catalyst, finding that positioning the catalyst downstream from a pulsed spark discharge discharge had a detrimental effect on both aromatic and hydrogen productivity. Without the catalyst at 623 K, a hydrogen yield of 62.6% was observed; however, the addition of the Ni/H-ZSM-5 catalyst resulted in a yield reduction of approximately 15–20%. This decline was attributed to the hydrogenolysis activity inherent to the nickel metal. Although increasing the reaction temperature beyond 673 K with the Ni-based catalyst did enhance hydrogen production, it simultaneously led to a significant escalation in coke formation [169].

Kasinathan et al. examined the impact of MgO/Al₂O₃ catalyst particle dimensions on methane activation within a dielectric barrier discharge (DBD) reactor. Their results indicated that reducing the particle size from 1.75 mm down to 0.25 mm led to a notable rise in methane conversion, which climbed from 9.5% to 23.0%. A corresponding improvement was observed in hydrogen productivity, with yields increasing as the catalyst size decreased. The researchers ascribed this heightened activity in smaller particles to the more efficient interface between the reactive plasma species and the catalytic surface, thereby emphasizing the critical importance of catalyst morphology in the conversion of CH₄ to H₂ [170].

In investigations of plasma-catalytic processes, the flow rate and composition of the gas feed are frequently adjusted as primary operational variables. For instance, Shuanghui et al. explored the impact of methane flow rates on the production of C₂ hydrocarbons and hydrogen in a gliding arc discharge system. They observed that as the flow rate increased from 14 to 66 mL/min, the methane conversion dropped from 81.28% to 59.66%, with a corresponding decrease in hydrogen yield. This

trend was attributed to the reduced residence time, which provides insufficient duration for the coupling of methyl and hydrogen radicals into the desired chemical products [171].

Ghanbari et al. examined how varying the applied voltage influenced methane conversion over a Ni–K₂O/Al₂O₃ catalyst within a nanosecond pulsed DBD plasma system. At an operating voltage of 8 kV, the integration of the catalyst enhanced methane conversion from 76.4% to 79.3% and boosted hydrogen production from 64.1% to 73.9% relative to the standalone plasma configuration. Furthermore, the presence of the Ni–K₂O/Al₂O₃ catalyst at this voltage enabled a reduction in discharge power from 162 W to 141.4 W—a nearly 10% decrease—while simultaneously improving the overall energy efficiency of the conversion process [172].

Plasma-catalytic processes emerge as a promising solution for on-demand hydrogen generation, offering a viable pathway to minimize greenhouse gas (GHG) footprints, especially when coupled with renewable energy sources like wind and solar power. Consequently, this technology is suitable for a broad spectrum of both mobile and stationary uses, ranging from sustainable power generation in fuel cells to specialized industrial sectors such as metallurgical processing, food hydrogenation, and semiconductor manufacturing. Furthermore, plasma catalysis can offer superior economic feasibility compared to traditional reforming techniques; its competitive capital expenditure requirements, suitability for modular and distributed deployment, and flexibility with diverse feedstocks make it an ideal candidate for establishing efficient on-site and on-board hydrogen supply systems [173].

Nevertheless, several persistent challenges continue to hinder the widespread adoption of plasma-catalysis for hydrogen generation. A critical concern remains the overall energy efficiency of these systems. In broad terms, energy efficiency represents the ratio between the energy content of the resulting product gas and the total energy consumption required for its production [174]. Currently, the energy efficiency levels documented for plasma-driven hydrocarbon reforming remain significantly lower than the benchmarks necessary for industrial-scale deployment. To illustrate, one of the peak efficiencies reported for plasma-assisted steam reforming reaches 60%, achieved at a methane conversion rate of 74% [175]. In DBD plasma-based reforming processes, the conversion of hydrocarbons, including methane, is typically associated with relatively low energy efficiency. However, the integration of catalytic materials with the plasma discharge has been shown to substantially enhance the overall energy efficiency of the process [176]. Early investigations employing a ferroelectric pellet-packed bed reactor demonstrated that hydrogen production from water could achieve an energy efficiency approximately one order of magnitude greater than that of photocatalytic methods. Nevertheless, the efficiency remained lower than that attainable through conventional water electrolysis [177]. The energy efficiency of plasma-assisted processes is strongly dependent on the type of plasma source utilized. Among the various plasma technologies investigated, microwave plasma has been reported to exhibit superior energy efficiency for CO₂ conversion under moderate-pressure conditions [178].

The elevated reduced electric fields characteristic of DBD plasmas promote electron-impact excitation and molecular bond dissociation, enabling reaction pathways that are otherwise energetically unfavorable. In plasma-catalytic systems, careful catalyst selection can further enhance energy efficiency by increasing process selectivity and product yield at a given energy input, as well as through catalyst polarization effects that locally intensify the electric field within packed-bed reactors. Furthermore, plasma-catalytic technologies offer the advantage of seamless integration with renewable energy sources. By

utilizing electricity generated from wind, solar, hydropower, wave, or tidal systems, these processes can provide a more sustainable route for plasma generation and hydrogen production [179].

Table 1. General comparison of plasma-assisted hydrogen production technologies with respect to plasma characteristics, hydrogen yield, energy efficiency, and practical applicability.

Method	Plasma Type	Main Energy Source	Typical Operating Conditions	Reported H ₂ Yield / Conversion	Energy Efficiency	Main Advantages	Main Limitations
LIP	Laser-induced plasma	Pulsed laser irradiation	Localized plasma generated by laser ablation; atmospheric or controlled atmosphere	Qualitative hydrogen generation reported from hydrocarbon decomposition	Not explicitly reported	Precise energy deposition, catalyst-assisted reactions, nanoparticle generation, controllable plasma chemistry	High laser cost, methane dissociation limited without catalysts, scalability challenges
SD-LIP	Hybrid warm plasma	Spark discharge + laser	Laser-triggered spark discharge with catalyst assistance	Enhanced methane and propane conversion; improved H ₂ production compared with conventional plasma methods	Reduced energy consumption relative to SD alone	Lower breakdown voltage, higher electron density, coke removal, catalyst self-cleaning, improved controllability	Requires laser system; industrial-scale efficiency still requires improvement
DBD	Non-thermal (cold plasma)	High-voltage AC/pulsed power	Atmospheric pressure, low temperature, kHz–MHz operation	H ₂ yield typically 30–40%	6–10%	Simple design, low operating temperature, easy catalyst integration, easy scale-up, versatile feedstocks	Relatively low energy efficiency and conversion
Corona Discharge	Non-thermal (cold plasma)	High-voltage AC/DC/pulsed DC	Atmospheric pressure; non-uniform electric field near sharp electrodes	Typical H ₂ yield ~56%; up to 70% reported in DRM	Typical ~10.7%; up to 14.3% reported	Simple reactor design, atmospheric-pressure operation, relatively high H ₂ yield in DRM	Small plasma volume, performance strongly depends on discharge polarity
GA/RGA	Warm plasma	AC or DC arc discharge	Atmospheric pressure; gliding or rotating arc sustained by gas flow	CH ₄ conversion up to 58.5%; H ₂ yield up to 20.7% reported	Relatively high (qualitative)	High gas throughput, higher energy efficiency than many non-thermal plasmas, improved residence time in RGA	Electrode deterioration, carbon deposition, short residence time in conventional GA
MW Plasma	Warm plasma	Microwave radiation (typically 2.45 GHz or 915 MHz)	Electrode-free discharge; atmospheric or reduced pressure	H ₂ yield 50–100%	24–47%	High conversion, high selectivity, large treatment volume, no electrode contamination, uniform energy deposition	Complex equipment and relatively high capital cost
RF Plasma	Warm/non-equilibrium plasma	Radio-frequency electromagnetic field (1–100 MHz)	Capacitive or inductive coupling; electrode-less operation possible	CH ₄ conversion 99.99 ± 0.06% reported in helicon plasma reactor	Not directly reported in article	Uniform large-volume plasma, electrode-less design, low gas temperature, solid carbon co-product instead of CO ₂	Lower energy efficiency than conventional SMR; complex RF power system
Plasma Catalysis	Hybrid plasma–catalyst system (commonly DBD-based)	Electrical discharge + catalyst	In-plasma catalysis (IPC) or post-plasma catalysis (PPC)	Significant improvement in CH ₄ conversion and H ₂ selectivity compared with plasma alone	Generally higher than plasma-only systems; catalyst reduced power demand by ~10% in reported study	Enhanced selectivity, lower activation barriers, improved energy efficiency, compatibility with renewable electricity	Mechanisms remain complex; catalyst deactivation and energy efficiency remain challenges

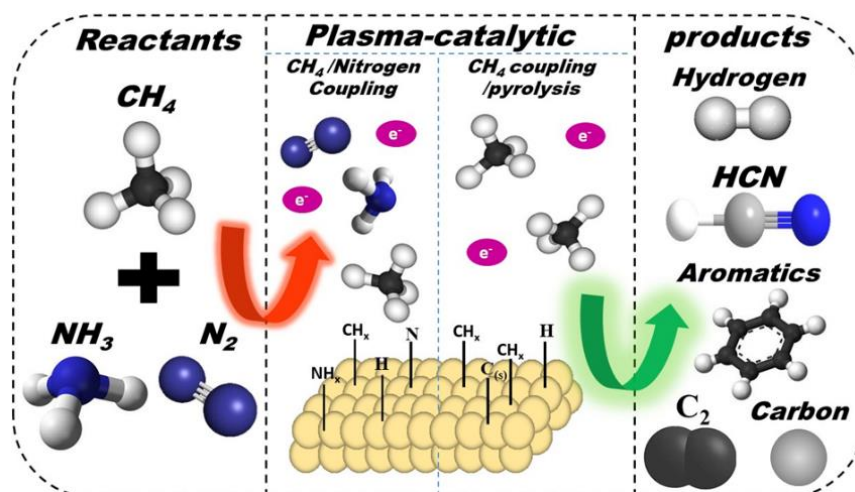


Fig. 9. Reaction pathways involved in plasma-catalytic hydrogen production from CH_4 , NH_3 , and N_2 , showing reactant coupling, catalyst-assisted pyrolysis, and the formation of H_2 , HCN , aromatic compounds, C_2 hydrocarbons, and solid carbon. Adapted from Ref. [3].

4. Conclusion

Despite the remarkable progress achieved in plasma-assisted hydrogen generation, several challenges still limit the large-scale implementation of these technologies. One of the most important issues is the relatively low energy efficiency of many plasma systems compared with conventional industrial processes. In addition, reactor optimization remains a critical task because plasma characteristics strongly depend on parameters such as power input, gas composition, pressure, reactor geometry, and catalyst configuration. Carbon deposition and catalyst deactivation are also significant concerns, particularly during the non-oxidative conversion of hydrocarbons, where coke formation can reduce reactor performance and operational stability over time.

Recent developments demonstrate that hybrid approaches can help overcome some of these limitations. In particular, the integration of plasma with catalysts has shown considerable potential for improving reactant conversion, hydrogen selectivity, and overall process efficiency. Similarly, advanced plasma configurations such as spark discharge-assisted laser-induced plasma (SD-LIP) offer promising solutions for suppressing coke formation, lowering breakdown voltage, and enhancing plasma controllability. Electrode-free systems, including microwave and radio-frequency plasmas, further provide attractive alternatives by eliminating electrode erosion and contamination issues.

Future research should focus on improving energy efficiency, understanding plasma–catalyst interactions, developing durable catalyst materials, and designing scalable reactor systems suitable for industrial operation. The increasing availability of renewable electricity also creates new opportunities for coupling plasma technologies with sustainable energy sources. With continued advances in reactor engineering, plasma diagnostics, and catalyst design, plasma-based hydrogen production is expected to play an increasingly important role in the transition toward clean and low-carbon energy systems.

Declaration of competing interest

The authors declare that they have no known competing financial interests or personal relationships that could have appeared to influence the work reported in this paper.

Data availability

No data is used in this article.

References

- [1] M. Liao, Y. Chen, Z. Cheng, C. Wang, X. Luo, and E. Bu, Hydrogen production from partial oxidation of propane: Effect of SiC addition on Ni/Al₂O₃ catalyst, *Appl. Energy* 252 (2019) 113435.
- [2] T. Ramantani, V. Evangelidou, G. Kormentzas, and D. I. Kondarides, Hydrogen production by steam reforming of propane and LPG over supported metal catalysts, *Appl. Catal. B Environ.* 306 (2022) 121129.
- [3] J. Y. Do, R. K. Chava, N. Son, J. Kim, N. Park, D. Lee, M. W. Seo, H. Ryu, J. H. Chi, and M. Kang, Effect of Ce Doping of a Co/Al₂O₃ Catalyst on Hydrogen Production via Propane Steam Reforming, *Catalysts* 8 (2018) 413.
- [4] N. Wang, H. O. Otor, G. Rivera-Castro, and J. C. Hicks, Plasma catalysis for hydrogen production: a bright future for decarbonization, *ACS Catal.* 14 (2024) 6749-6798.
- [5] P. Bains, S. Bennett, L. Collina, E. Connelly, C. Delmastro, S. Evangelopoulou, M. Fajardy, A. Gouy, M. Kotani, J. Le Marois, and P. Levi, Global hydrogen review 2023, International Energy Agency, Paris, France, 2023.
- [6] I. Dincer and C. Acar, Review and evaluation of hydrogen production methods for better sustainability, *Int. J. Hydrogen Energy* 40 (2014) 11094-11111.
- [7] M. J. Cook, T. Nott, W. J. Trompeter, J. Futter, C. W. Bumby, and J. V. Kennedy, Plasma mediated water splitting for hydrogen production, *J. Phys. Energy* 7 (2025) 022002.
- [8] I. Adamovich, S. D. Baalrud, A. Bogaerts, P. J. Bruggeman, M. Cappelli, V. Colombo, U. Czarnetzki, U. Ebert, J. G. Eden, P. Favia, D. B. Graves, S. Hamaguchi, G. Hieftje, M. Hori, I. D. Kaganovich, U. Kortshagen, M. J. Kushner, N. J. Mason, S. Mazouffre, S. Mededovic Thagard, H.-R. Metelmann, A. Mizuno, E. Moreau, A. B. Murphy, B. A. Niemira, G. S. Oehrlein, Z. Lj. Petrovic, L. C. Pitchford, Y.-K. Pu, S. Rauf, O. Sakai, S. Samukawa, S. Starikovskaia, J. Tennyson, K. Terashima, M. M. Turner, M. C. M. van de Sanden, and A. Vardelle, The 2017 plasma roadmap: low temperature plasma science and technology, *J. Phys. D: Appl. Phys.* 50 (2017) 323001.
- [9] D. C. Walker and R. A. Back, Photochemistry in the Photo-Ionization Region. II. Photochemistry of Methane, Ethane, and Ethylene at Wavelengths below 900, *J. Chem. Phys.* 38 (1963) 1526-1535.
- [10] E. M. Magee, Photolysis of Methane by Vacuum-Ultraviolet Light, *J. Chem. Phys.* 39 (1963) 855-858.
- [11] A. R. Derk, H. H. Funke, and J. L. Falconer, Methane conversion to higher hydrocarbons by UV irradiation, *Ind. Eng. Chem. Res.* 47 (2008) 6568-6572.
- [12] C. M. Kalamaras and A. M. Efstathiou, Hydrogen Production Technologies: Current State and Future Developments, *Conf. Pap. Energy* (2013) 1-9.
- [13] Z. Ghorbani, P. Parvin, A. Reyhani, S. Z. Mortazavi, A. Moosakhani, M. Maleki, and S. Kiani, Methane decomposition using metal-assisted nanosecond laser induced plasma at atmospheric pressure, *J. Phys. Chem. C* 118 (2014) 29822-29835.
- [14] M. Habibpour, P. Parvin, and R. Amrollahi, Gold fineness measurement using single-shot spark assisted laser-induced breakdown spectroscopy, *Appl. Opt.* 60 (2021) 1099.
- [15] A. Moosakhani, P. Parvin, A. Reyhani, and S. Z. Mortazavi, Propane decomposition and conversion into other hydrocarbons using metal target assisted laser induced plasma, *Phys. Plasmas* 24 (2017) 013505.
- [16] F. Ahmadiouri and P. Parvin, Methane conversion using spark discharge-assisted laser-induced plasma (SD-LIP) with Pd catalyst: non-oxidative hydrogen production, *Chem. Eng. J.* 484 (2024) 149645.
- [17] F. Ahmadiouri and P. Parvin, Non-oxidative conversion of propane by employing laser-triggered spark discharge: effective hydrogen production, *Energy Convers. Manage.* 347 (2026) 120555.
- [18] F. Ahmadiouri, P. Parvin, R. Hosseini, Z. Zare, and A. R. Rabbani, Effective methane decomposition using spark discharge assisted laser-induced plasma: an approach based on Fourier transform infrared (FTIR) spectroscopy, *Spectrochim. Acta Part A Mol. Biomol. Spectrosc.* 326 (2025) 125257.
- [19] F. Ghasemi, P. Parvin, J. Reif, S. Abachi, M. R. Mohebbifar, and M. R. Razzaghi, Laser induced breakdown spectroscopy for the diagnosis of several malignant tissue samples, *J. Laser Appl.* 29 (2017) 042005.
- [20] A. Moosakhani, P. Parvin, S. Z. Mortazavi, A. Reyhani, and S. Abachi, Effect of hydrocarbon molecular decomposition on palladium-assisted laser-induced plasma ablation, *Appl. Opt.* 56 (2017) 11.
- [21] P. Parvin, H. R. Dehghanpour, M. M. Faani, A. Bavali, F. Ahmadiouri, and S. Ebrahimnasab, LIF/LIB spectroscopy of crude oil-saturated carbonate bedrock, *Phys. Scr.* 98 (2023) 105410.
- [22] P. Mohammadimatin, P. Parvin, A. Jafargohli, A. Jahanbakhshi, F. Ahmadiouri, A. Tabibkhomei, O. Heidari, and S. Salarinejad, Signal enhancement in spark-assisted laser-induced breakdown spectroscopy for discrimination of glioblastoma and oligodendroglioma lesions, *Biomed. Opt. Express* 14 (2023) 5795-5816.
- [23] J. S. Chang, P. A. Lawless, and T. Yamamoto, Corona discharge processes, *IEEE Trans. Plasma Sci.* 19 (1991) 1152-1166.
- [24] B. Eliasson and U. Kogelschatz, Non equilibrium volume plasma chemical processing, *IEEE Trans. Plasma Sci.* 19 (1991) 1063-1077.
- [25] J.-J. Zou, Y.-P. Zhang, and C.-J. Liu, Hydrogen production from dimethyl ether using corona discharge plasma, *J. Power Sources* 163 (2007) 653-657.
- [26] C. Tendero, C. Tixier, P. Tristant, J. Desmaison, and P. Leprince, Atmospheric pressure plasmas: A review, *Spectrochim. Acta Part B* 61 (2006) 2-30.
- [27] M. Jasiński, M. Dors, and J. Mizeraczyk, Production of hydrogen via methane reforming using atmospheric pressure microwave plasma, *J. Power Sources* 181 (2008) 41-45.
- [28] M. Jasiński, M. Dors, and J. Mizeraczyk, Application of atmospheric pressure microwave plasma source for production of hydrogen via methane reforming, *Eur. Phys. J. D* 54 (2009) 179-183.

- [29] M. Jasiński, M. Dors, H. Nowakowska, G. V. Nichipor, and J. Mizeraczyk, Production of hydrogen via conversion of hydrocarbons using a microwave plasma, *J. Phys. D: Appl. Phys.* 44 (2011) 194002.
- [30] M. Jasiński, D. Czyłkowski, B. Hrycak, M. Dors, and J. Mizeraczyk, Atmospheric pressure microwave plasma source for hydrogen production, *Int. J. Hydrogen Energy* 38 (2013) 11473-11483.
- [31] D. Czyłkowski, B. Hrycak, M. Jasiński, M. Dors, and J. Mizeraczyk, Microwave plasma-based method of hydrogen production via combined steam reforming of methane, *Energy* 113 (2016) 653-661.
- [32] M. A. Lieberman and A. J. Lichtenberg, Principles of Plasma Discharges and Materials Processing, *MRS Bull.* 30 (2005) 899-901.
- [33] A. E. E. Putra, S. Nomura, S. Mukasa, and H. Toyota, Hydrogen production by radio frequency plasma stimulation in methane hydrate at atmospheric pressure, *Int. J. Hydrogen Energy* 37 (2012) 16000-16005.
- [34] U. Kogelschatz, Dielectric-barrier discharge: Their history, discharge physics, and industrial applications, *Plasma Chem. Plasma Process.* 23 (2003) 1-46.
- [35] Y. Zeng, X. Zhu, D. Mei, B. Ashford, and X. Tu, Plasma-catalytic dry reforming of methane over γ -Al₂O₃ supported metal catalysts, *Catal. Today* 256 (2015) 80-87.
- [36] A. Czernichowski, Gliding arc: Application to engineering and environmental control, *Pure Appl. Chem.* 66 (1994) 1301-1310.
- [37] C. S. Kalra, Y. I. Cho, A. Gutsol, A. Fridman, and T. S. Rufael, Gliding arc in tornado using a reverse vortex flow, *Rev. Sci. Instrum.* 76 (2005) 025110.
- [38] S. P. Gangoli, Experimental and modeling study of warm plasmas and their applications, Ph.D. dissertation, Drexel University, Philadelphia, PA, 2007.
- [39] C. S. Kalra, A. F. Gutsol, and A. A. Fridman, Gliding arc discharges as a source of intermediate plasma for methane partial oxidation, *IEEE Trans. Plasma Sci.* 33 (2005) 32-41.
- [40] I. Rusu and J. M. Cormier, On a possible mechanism of the methane steam reforming in a gliding arc reactor, *Chem. Eng. J.* 91 (2003) 23-31.
- [41] D. H. Lee, K. T. Kim, M. S. Cha, and Y. H. Song, Plasma-controlled chemistry in plasma reforming of methane, *Int. J. Hydrogen Energy* 35 (2010) 10967-10976.
- [42] H. Nazir, N. Muthuswamy, C. Louis, S. Jose, J. Prakash, M. E. M. Buan, C. Flox, S. Chavan, X. Shi, P. Kauranen, T. Kallio, G. Maia, K. Tammeveski, N. Lymperopoulos, E. Carcadea, E. Veziroglu, A. Iranzo, and A. M. Kannan, Is the H₂ Economy Realizable in the Foreseeable Future? Part I: H₂ Production Methods, *Int. J. Hydrogen Energy* 45 (2020) 13777-13788.
- [43] W. G. Mixer, ART. VIII.—on Electrosynthesis: Carbonic Oxide and Oxygen. Methane and Oxygen. Ethylene and Oxygen. Acetylene and Oxygen. Ethane and Oxygen. *Molecular Changes, Am. J. Sci.* 4 (1897) 51.
- [44] H. M. Mott-Smith, History of "Plasmas", *Nature* 233 (1971) 219.
- [45] Y. Xu, X. Bao, and L. Lin, Direct conversion of methane under nonoxidative conditions, *J. Catal.* 216 (2003) 386-395.
- [46] S. Z. Mortazavi, P. Parvin, A. Reyhani, and S. Mirershadi, Hydrogen storage property of laser induced Pd nanoparticle decorated multi-walled carbon nanotubes, *RSC Adv.* 3 (2013) 1397.
- [47] M. Mehrabi, P. Parvin, A. Reyhani, and S. Z. Mortazavi, Hybrid laser ablation and chemical reduction to synthesize Ni/Pd nanoparticles decorated multi-wall carbon nanotubes for effective enhancement of hydrogen storage, *Int. J. Hydrogen Energy* (2018) 1-11.
- [48] M. Mehrabi, A. Reyhani, P. Parvin, and S. Z. Mortazavi, Surface structural alteration of multi-walled carbon nanotubes decorated by nickel nanoparticles based on laser ablation/chemical reduction methods to enhance hydrogen storage properties, *Int. J. Hydrogen Energy* 44 (2019) 3812-3823.
- [49] J. F. Ready, Effects of High-Power Laser Radiation, Academic Press, New York, 1971, pp. 161-208.
- [50] L. Radziemski and D. Cremers, A brief history of Laser-Induced Breakdown Spectroscopy: From the concept of atoms to LIBS 2012, *Spectrochim. Acta Part B* 87 (2013) 3-10.
- [51] A. W. Miziolek, V. Palleschi, and I. Schechter, Laser-induced Breakdown Spectroscopy (LIBS): Fundamentals and Applications, Cambridge University Press, Cambridge, UK, 2006.
- [52] W. Sdorra and K. Niemax, *Microchim. Acta* 107 (1992) 319.
- [53] A. J. Ball, V. Hohreiter, and D. W. Hahn, *Appl. Spectrosc.* 59 (2005) 348.
- [54] T. M. Khan and T. BiBi, Application of NS Pulsed Laser Ablation for Dense CdS Nanoparticles Deposition in Argon Atmosphere, *SOP Trans. Appl. Phys.* 1 (2014) 48-54.
- [55] W. W. Stoffels, E. Stoffels, G. Ceccone, and F. Rossi, Laser-induced particle formation and coalescence in a methane discharge, *J. Vac. Sci. Technol. A* 17 (1999) 3385-3392.
- [56] M. Stafe, A. Marcu, and N. N. Puscas, Pulsed Laser Ablation of Solids (Basics, Theory and Applications), Springer, Heidelberg, 2014.
- [57] D. Bäuerle, Laser chemical processing: an overview to the 30th anniversary, *Appl. Phys. A* 101 (2010) 447-459.
- [58] J. P. Matte, M. Lamoureux, C. Moller, R. Y. Yin, J. Delettrez, J. Vermont, and T. W. Johnston, Non-Maxwellian electron distribution and continuum X-ray emission in inverse Bremsstrahlung heated plasmas, *Plasma Phys. Controlled Fusion* 30 (1988) 1665-1689.
- [59] D. A. Cremers and L. J. Radziemski, Handbook of Laser-Induced Breakdown Spectroscopy, John Wiley and Sons, New York, 2006.
- [60] S. Z. Mortazavi, P. Parvin, A. Reyhani, A. N. Golikand, and S. Mirershadi, Effect of Laser Wavelength at IR (1064 nm) and UV (193 nm) on the Structural Formation of Palladium Nanoparticles in Deionized Water, *J. Phys. Chem. C* 115 (2011) 5049-5057.
- [61] S. Z. Mortazavi, P. Parvin, M. R. MousaviPour, A. Reyhani, A. Moosakhani, and S. Moradkhani, Time-resolved evolution of metal plasma induced by Q-switched Nd:YAG and ArF-excimer lasers, *Opt. Laser Technol.* 62 (2014) 32-39.
- [62] N. N. Nedialkov, S. E. Imamova, P. A. Atanasov, P. Berger, and F. Dausinger, Mechanism of ultrashort laser ablation of metals: molecular dynamics simulation, *Appl. Surf. Sci.* 247 (2005) 243-248.
- [63] L. Juha and S. Civiš, Lasers in Chemistry, in: Encyclopedia of Applied Physics, Wiley-VCH, Weinheim, 2008, pp. 899-921.
- [64] H. P. Graf, M. W. Sigrist, and F. K. Kneubühl, *Helv. Phys. Acta* 52 (1979) 56-60.
- [65] B. A. Sayyed and P. C. Stair, *J. Phys. Chem.* 94 (1990) 409-414.

- [66] H. B. Bebb and A. Gold, Multiphoton Ionization of Hydrogen and Rare-Gas Atoms, *Phys. Rev.* 143 (1966) 1-24.
- [67] M. D. Perry, O. L. Landen, A. Szoke, and E. M. Campbell, Multiphoton ionization of the noble gases by an intense 10^{14} -W/cm² dye laser, *Phys. Rev. A* 37 (1988) 747-760.
- [68] G. B. Zhao, S. John, J. J. Zhang, L. Wang, S. Muknahallipatna, J. C. Hamann, J. F. Ackerman, M. D. Argyle, and O. A. Plumb, Methane conversion in pulsed corona discharge reactors, *Chem. Eng. J.* 125 (2006) 67-79.
- [69] A. B. Redondo, E. Troussard, and J. A. Van Bokhoven, Non-oxidative methane conversion assisted by corona discharge, *Fuel Process. Technol.* 104 (2012) 265-270.
- [70] S. Y. Liu, D. H. Mei, Z. Shen, and X. Tu, Nonoxidative conversion of methane in a dielectric barrier discharge reactor: Prediction of reaction performance based on neural network model, *J. Phys. Chem. C* 118 (2014) 10686-10693.
- [71] F. Saleem, J. Kennedy, U. H. Dahiru, K. Zhang, and A. Harvey, Methane conversion to H₂ and higher hydrocarbons using non-thermal plasma dielectric barrier discharge reactor, *Chem. Eng. Process. - Process Intensif.* 142 (2019) 107557.
- [72] A. Indarto, J.-W. Choi, H. Lee, and H. K. Song, Effect of additive gases on methane conversion using gliding arc discharge, *Energy* 31 (2006) 2986-2995.
- [73] H. Sun, Non-oxidative methane conversion in diffuse, filamentary, and spark regimes of nanosecond repetitively pulsed discharge with negative polarity, *Plasma Process. Polym.* 16 (2019) 1-15.
- [74] Y. Gao, S. Zhang, H. Sun, R. Wang, X. Tu, and T. Shao, Highly efficient conversion of methane using microsecond and nanosecond pulsed spark discharges, *Appl. Energy* 226 (2018) 534-545.
- [75] W. Cho, Y. Baek, S. K. Moon, and Y. C. Kim, Oxidative coupling of methane with microwave and RF plasma catalytic reaction over transitional metals loaded on ZSM-5, *Catal. Today* 74 (2002) 207-223.
- [76] M. Heintze and M. Magureanu, Methane conversion into acetylene in a microwave plasma: Optimization of the operating parameters, *J. Appl. Phys.* 92 (2002) 2276-2283.
- [77] M. Caetano and P. Patin, Coupling and reforming of methane by means of low pressure radio-frequency plasmas, *Fuel* 84 (2014) 2008-2014.
- [78] B. Wanten, S. Maerivoet, C. Vantomme, J. Slaets, G. Trenchev, and A. Bogaerts, Dry reforming of methane in an atmospheric pressure glow discharge: Confining the plasma to expand the performance, *J. CO₂ Util.* 56 (2022) 101869.
- [79] R. Lotfalipour, A. M. Ghorbanzadeh, and A. Mahdian, Methane conversion by repetitive nanosecond pulsed plasma, *J. Phys. D: Appl. Phys.* 47 (2014) 365201.
- [80] X. Wang, Y. Gao, S. Zhang, H. Sun, J. Li, and T. Shao, Nanosecond pulsed plasma assisted dry reforming of CH₄: The effect of plasma operating parameters, *Appl. Energy* 243 (2019) 132-144.
- [81] A. Voloshko, J.-P. Colombier, and T. E. Itina, Comparison of laser ablation with spark discharge techniques used for nanoparticle production, *Appl. Surf. Sci.* 336 (2014) 143-149.
- [82] A. Voloshko and T. E. Itina, Nanoparticle Formation by Laser Ablation and by Spark Discharges — Properties, Mechanisms, and Control Possibilities, in: *Nanoparticles Technology*, Chapter 1, 2015.
- [83] A. Fridman, *Plasma Chemistry*, Cambridge University Press, New York, 2008.
- [84] M. E. Abdel-kader, W. H. Gaber, F. A. Ebrahim, and M. A. Abd Al-Halim, Characterization of the electrical breakdown for DC discharge in Ar-He gas mixture, *Vacuum* 169 (2019) 108922.
- [85] M. V. Belkov, V. S. Burakov, A. De Giacomo, V. V. Kiris, S. N. Raikov, and N. V. Tarasenko, Comparison of two laser-induced breakdown spectroscopy techniques for total carbon measurement in soils, *Spectrochim. Acta B* 64 (2009) 899-904.
- [86] W. Zhou, K. Li, H. Qian, Z. Ren, and Y. Yu, Effect of voltage and capacitance in nanosecond pulse discharge enhanced laser-induced breakdown spectroscopy, *Appl. Opt.* 51 (2012) B42-B48.
- [87] Y. Wang, Y. Jiang, X. He, Y. Chen, and R. Li, Triggered parallel discharge in laser-ablation spark-induced breakdown spectroscopy and studies on its analytical performance for aluminum and brass samples, *Spectrochim. Acta B* 150 (2018) 9-17.
- [88] M. M. Hassanimatin, S. H. Tavassoli, Y. Nosrati, and A. Safi, A combination of electrical spark and laser-induced breakdown spectroscopy on a heated sample, *Phys. Plasmas* 26 (2019) 033303.
- [89] D. P. Subedi, U. M. Joshi, and C. S. Wong, *Dielectric Barrier Discharge (DBD) Plasmas and Their Applications*, in: *Plasma Science and Technology for Emerging Economies: An AAAPT Experience*, Springer, 2017, pp. 693-737.
- [90] K. P. Francke, R. Rudolph, and H. Miessner, Design and Operating Characteristics of a Simple and Reliable DBD Reactor for Use with Atmospheric Air, *Plasma Chem. Plasma Process.* 23 (2003) 47-57.
- [91] J. He, X. Wen, L. Wu, H. Chen, J. Hu, and X. Hou, Dielectric Barrier Discharge Plasma for Nanomaterials: Fabrication, Modification and Analytical Applications, *TrAC-Trends Anal. Chem.* 156 (2022) 116715.
- [92] R. Brandenburg, Corrigendum: Dielectric Barrier Discharges: Progress on Plasma Sources and on the Understanding of Regimes and Single Filaments, *Plasma Sources Sci. Technol.* 27 (2018) 079501.
- [93] K. Ollegott, P. Wirth, C. Oberste-Beulmann, P. Awakowicz, and M. Muhler, Fundamental Properties and Applications of Dielectric Barrier Discharges in Plasma-Catalytic Processes at Atmospheric Pressure, *Chem.-Ing.-Tech.* 92 (2020) 1542-1558.
- [94] A. Chirokov, A. Gutsol, and A. Fridman, Atmospheric Pressure Plasma of Dielectric Barrier Discharges, *Pure Appl. Chem.* 77 (2005) 487-495.
- [95] T. N. Jukes and K. S. Choi, On the Formation of Streamwise Vortices by Plasma Vortex Generators, *J. Fluid Mech.* 733 (2013) 370-393.
- [96] T. Von Woedtke, M. Laroussi, and M. Gherardi, Foundations of Plasmas for Medical Applications, *Plasma Sources Sci. Technol.* 31 (2022) 054002.
- [97] W. Lu, Y. Abbas, M. F. Mustafa, C. Pan, and H. Wang, A Review on Application of Dielectric Barrier Discharge Plasma Technology on the Abatement of Volatile Organic Compounds, *Front. Environ. Sci. Eng.* 13 (2019) 1-19.
- [98] F. Peeters and T. Butterworth, Electrical Diagnostics of Dielectric Barrier Discharges, in: *Atmospheric Pressure Plasma - from Diagnostics to Applications*, 2019, pp. 23-49.
- [99] E. E. Kunhardt, Generation of Large-Volume, Atmospheric Pressure, Nonequilibrium Plasmas, *IEEE Trans. Plasma Sci.* 28 (2000) 189-200.

- [100] J. Li, C. Ma, S. Zhu, F. Yu, B. Dai, and D. Yang, A Review of Recent Advances of Dielectric Barrier Discharge Plasma in Catalysis, *Nanomaterials* 9 (2019) 1428.
- [101] D. Mei and X. Tu, Conversion of CO₂ in a Cylindrical Dielectric Barrier Discharge Reactor: Effects of Plasma Processing Parameters and Reactor Design, *J. CO₂ Util.* 19 (2017) 68-78.
- [102] R. Snoeckx, Y. X. Zeng, X. Tu, and A. Bogaerts, Plasma-Based Dry Reforming: Improving the Conversion and Energy Efficiency in a Dielectric Barrier Discharge, *RSC Adv.* 5 (2015) 29799-29808.
- [103] J. Coogan and A. Sappey, Distribution of OH within silent discharge plasma reactors, *IEEE Trans. Plasma Sci.* 24 (1996) 91-92.
- [104] A. H. Khoja, M. Tahir, and N. A. S. Amin, Recent Developments in Non-Thermal Catalytic DBD Plasma Reactor for Dry Reforming of Methane, *Energy Convers. Manag.* 183 (2019) 529-560.
- [105] Y. Li, G. Xu, C. Liu, B. Eliasson, and B. Xue, Co-Generation of Syngas and Higher Hydrocarbons from CO₂ and CH₄ Using Dielectric-Barrier Discharge: Effect of Electrode Materials, *Energy Fuels* 15 (2001) 299-302.
- [106] D. Ray, P. M. K. Reddy, and C. Subrahmanyam, Glass Beads Packed DBD-Plasma Assisted Dry Reforming of Methane, *Top. Catal.* 60 (2017) 869-878.
- [107] W. Wang, H. H. Kim, K. Van Laer, and A. Bogaerts, Streamer Propagation in a Packed Bed Plasma Reactor for Plasma Catalysis Applications, *Chem. Eng. J.* 334 (2018) 2467-2479.
- [108] Z. Sheng, S. Kameshima, K. Sakata, and T. Nozaki, Plasma Enabled Dry Methane Reforming, in: *Plasma Chemistry and Gas Conversion*, Chapter 3, 2018.
- [109] H.-H. Kim, Y. Teramoto, and A. Ogata, Time-Resolved Imaging of Positive Pulsed Corona-Induced Surface Streamers on TiO₂ and γ-Al₂O₃-Supported Ag Catalysts, *J. Phys. D: Appl. Phys.* 49 (2016) 415204.
- [110] Q. Wang, B. H. Yan, Y. Jin, and Y. Cheng, Investigation of Dry Reforming of Methane in a Dielectric Barrier Discharge Reactor, *Plasma Chem. Plasma Process.* 29 (2009) 217-228.
- [111] A. Bogaerts, X. Tu, and G. Van Rooij, Plasma-Based CO₂ Conversion, in: *Carbon Dioxide Utilisation: Transformations*, De Gruyter, 2019, pp. 585-634.
- [112] A. H. Khoja, M. Tahir, and N. A. S. Amin, Dry Reforming of Methane Using Different Dielectric Materials and DBD Plasma Reactor Configurations, *Energy Convers. Manag.* 144 (2017) 262-274.
- [113] Y. Uytendhouwen, J. Hereijgers, T. Breugelmans, P. Cool, and A. Bogaerts, How Gas Flow Design Can Influence the Performance of a DBD Plasma Reactor for Dry Reforming of Methane, *Chem. Eng. J.* 405 (2021) 126618.
- [114] X. Tu and J. C. Whitehead, Plasma-catalytic dry reforming of methane in an atmospheric dielectric barrier discharge: Understanding the synergistic effect at low temperature, *Appl. Catal. B Environ.* 125 (2012) 439-448.
- [115] H. L. Chen, H. M. Lee, S. H. Chen, Y. Chao, and M. B. Chang, Review of plasma catalysis on hydrocarbon reforming for hydrogen production—Interaction, integration, and prospects, *Appl. Catal. B* 85 (2008) 1-9.
- [116] R. Aerts, W. Somers, and A. Bogaerts, Carbon Dioxide Splitting in a Dielectric Barrier Discharge Plasma: A Combined Experimental and Computational Study, *ChemSusChem* 8 (2015) 702-716.
- [117] B. Eliasson, M. Hirth, and U. Kogelschatz, Ozone synthesis from oxygen in dielectric barrier discharges, *J. Phys. D: Appl. Phys.* 20 (1987) 1421-1437.
- [118] R. Snoeckx and A. Bogaerts, Plasma Technology - a Novel Solution for CO₂ Conversion?, *Chem. Soc. Rev.* 46 (2017) 5805-5863.
- [119] H. Taghvaei and M. R. Rahimpour, Upgrading of Anisole Using: In Situ Generated Hydrogen in Pin to Plate Pulsed Corona Discharge, *RSC Adv.* 6 (2016) 98369-98380.
- [120] M. Li, G. Xu, Y. Tian, L. Chen, and H. Fu, Carbon Dioxide Reforming of Methane Using DC Corona Discharge Plasma Reaction, *J. Phys. Chem. A* 108 (2004) 1687-1693.
- [121] M. W. Li, Y. L. Tian, and G. H. Xu, Characteristics of Carbon Dioxide Reforming of Methane via Alternating Current (AC) Corona Plasma Reactions, *Energy Fuels* 21 (2007) 2335-2339.
- [122] J. Feng, X. Sun, Z. Li, X. Hao, M. Fan, P. Ning, and K. Li, Plasma-Assisted Reforming of Methane, *Adv. Sci.* 9 (2022) 1-36.
- [123] A. Fridman, A. Chirokov, and A. Gutsol, Non-Thermal Atmospheric Pressure Discharges, *J. Phys. D: Appl. Phys.* 38 (2005) R1.
- [124] S. R. Sun, H. X. Wang, D. H. Mei, X. Tu, and A. Bogaerts, CO₂ Conversion in a Gliding Arc Plasma: Performance Improvement Based on Chemical Reaction Modeling, *J. CO₂ Util.* 17 (2017) 220-234.
- [125] W. Wang, D. Mei, X. Tu, and A. Bogaerts, Gliding Arc Plasma for CO₂ Conversion: Better Insights by a Combined Experimental and Modelling Approach, *Chem. Eng. J.* 330 (2017) 11-25.
- [126] F. G. M. de Medeiros, F. W. B. Lopes, and B. R. de Vasconcelos, Prospects and Technical Challenges in Hydrogen Production through Dry Reforming of Methane, *Catalysts* 12 (2022) 363.
- [127] Z. Bo, J. Yan, X. Li, Y. Chi, and K. Cen, Plasma Assisted Dry Methane Reforming Using Gliding Arc Gas Discharge: Effect of Feed Gases Proportion, *Int. J. Hydrogen Energy* 33 (2008) 5545-5553.
- [128] F. Zhu, H. Zhang, X. Yan, J. Yan, M. Ni, X. Li, and X. Tu, Plasma-Catalytic Reforming of CO₂-Rich Biogas over Ni/γ-Al₂O₃ Catalysts in a Rotating Gliding Arc Reactor, *Fuel* 199 (2017) 430-437.
- [129] N. Lu, D. Sun, Y. Xia, K. Shang, B. Wang, N. Jiang, J. Li, and Y. Wu, Dry Reforming of CH₄-CO₂ in AC Rotating Gliding Arc Discharge: Effect of Electrode Structure and Gas Parameters, *Int. J. Hydrogen Energy* 43 (2018) 13098-13109.
- [130] D. K. Dinh, G. Trenchev, D. H. Lee, and A. Bogaerts, Arc Plasma Reactor Modification for Enhancing Performance of Dry Reforming of Methane, *J. CO₂ Util.* 42 (2020) 101352.
- [131] H. Kwon, T. Kim, and S. Song, Dry Reforming of Methane in a Rotating Gliding Arc Plasma: Improving Efficiency and Syngas Cost by Quenching Product Gas, *J. CO₂ Util.* 70 (2023) 102448.
- [132] A. Fridman, S. Nester, L. A. Kennedy, A. Saveliev, and O. Mutaf-Yardimci, Gliding Arc Discharge, *Prog. Energy Combust. Sci.* 25 (1999) 211-231.

- [133] M. Birau, M. A. Krasil'nikov, M. V. Kuzlev, and A. A. Rukhadze, Nonlinear Theory of a Plasma Microwave Oscillator Using Cable Waves, *J. Exp. Theor. Phys.* 84 (1997) 694-702.
- [134] G. Chen, V. Georgieva, T. Godfroid, R. Snyders, and M. P. Delplanck-Ogletree, Plasma Assisted Catalytic Decomposition of CO₂, *Appl. Catal. B Environ.* 190 (2016) 115-124.
- [135] Y. Kim, M. Lee, and Y. J. Kim, Selective Growth and Contact Gap Fill of Low Resistivity Si via Microwave Plasma-Enhanced CVD, *Micromachines* 10 (2019) 689.
- [136] J. Ehlbeck, U. Schnabel, M. Polak, J. Winter, T. Von Woedtke, R. Brandenburg, T. Von Dem Hagen, and K. D. Weltmann, Low Temperature Atmospheric Pressure Plasma Sources for Microbial Decontamination, *J. Phys. D: Appl. Phys.* 44 (2011) 013002.
- [137] H. S. Uhm, Y. C. Hong, and D. H. Shin, A Microwave Plasma Torch and Its Applications, *Plasma Sources Sci. Technol.* 15 (2006) S26.
- [138] A. A. Zamri, M. Y. Ong, S. Nomanbhay, and P. L. Show, Microwave Plasma Technology for Sustainable Energy Production and the Electromagnetic Interaction within the Plasma System: A Review, *Environ. Res.* 197 (2021) 111204.
- [139] J. Q. Zhang, J. S. Zhang, Y. J. Yang, and Q. Liu, Oxidative Coupling and Reforming of Methane with Carbon Dioxide Using a Pulsed Microwave Plasma under Atmospheric Pressure, *Energy Fuels* 17 (2003) 54-59.
- [140] Y. F. Wang, C. H. Tsai, W. Y. Chang, and Y. M. Kuo, Methane Steam Reforming for Producing Hydrogen in an Atmospheric Pressure Microwave Plasma Reactor, *Int. J. Hydrogen Energy* 35 (2010) 135-140.
- [141] B. Hrycak, J. Mizeraczyk, D. Czykowski, M. Dors, M. Budnarowska, and M. Jasiński, Hydrogen Production by the Steam Reforming of Synthetic Biogas in Atmospheric-Pressure Microwave (915 MHz) Plasma, *Sci. Rep.* 13 (2023) 1-15.
- [142] I. Rahim, S. Nomura, S. Mukasa, and H. Toyota, Decomposition of Methane Hydrate for Hydrogen Production Using Microwave and Radio Frequency In-Liquid Plasma Methods, *Appl. Therm. Eng.* 90 (2015) 120-126.
- [143] Q. Wang, T. Zhu, Z. Li, X. Zhu, J. Liu, and B. Sun, Plasma Activation of Methane for Hydrogen in Microwave Liquid Discharge by Auxiliary Gases: A Way to Realize Efficient Utilization of Resources, *Fuel* 330 (2022) 125673.
- [144] M. Scapinello, E. Delikonstantis, and G. D. Stefanidis, The Panorama of Plasma-Assisted Non-Oxidative Methane Reforming, *Chem. Eng. Process. Process Intensif.* 117 (2017) 120-140.
- [145] H. Motz and C. J. H. Watson, The Radio-Frequency Confinement and Acceleration of Plasmas, *Adv. Electron. Electron Phys.* 23 (1967) 153-302.
- [146] K. S. Kim and T. H. Kim, Nanofabrication by thermal plasma jets: From nanoparticles to low-dimensional nanomaterials, *J. Appl. Phys.* 125 (2019) 070901.
- [147] H. Conrads and M. Schmidt, Plasma generation and plasma sources, *Plasma Sources Sci. Technol.* 9 (2000) 441-454.
- [148] S. Li, P. Arun, H. van den Bogaard, T. van Raak, C. Liu, and F. Gallucci, A review of experimental approaches, trends and opportunities in plasma-based gas conversion research, *Front. Chem. Sci. Eng.* 19 (2025) 96.
- [149] B. W. Longmier, A. D. Gallimore, and N. Hershkowitz, Hydrogen production from methane using an RF plasma source in total nonambipolar flow, *Plasma Sources Sci. Technol.* 21 (2012) 015007.
- [150] S. Nomura, S. Mukasa, H. Toyota, H. Miyake, H. Yamashita, T. Maehara, A. Kawashima, and F. Abe, Characteristics of in-liquid plasma in water under higher pressure than atmospheric pressure, *Plasma Sources Sci. Technol.* 20 (2011) 034012.
- [151] B. Loenders, R. Michiels, and A. Bogaerts, Is a Catalyst Always Beneficial in Plasma Catalysis? Insights from the Many Physical and Chemical Interactions, *J. Energy Chem.* 85 (2023) 501-533.
- [152] E. C. Neyts and A. Bogaerts, Understanding Plasma Catalysis through Modelling and Simulation - A Review, *J. Phys. D: Appl. Phys.* 47 (2014) 224010.
- [153] J. Hong, W. Chu, P. A. Chernavskii, and A. Y. Khodakov, Cobalt Species and Cobalt-Support Interaction in Glow Discharge Plasma Assisted Fischer-Tropsch Catalysts, *J. Catal.* 273 (2010) 9-17.
- [154] R. Martínez, E. Romero, C. Guimon, and R. Bilbao, CO₂ Reforming of Methane over Coprecipitated Ni-Al Catalysts Modified with Lanthanum, *Appl. Catal. A Gen.* 274 (2004) 139-149.
- [155] K. Ostrikov, E. C. Neyts, and M. Meyyappan, Plasma Nanoscience: From Nano-Solids in Plasmas to Nano-Plasmas in Solids, *Adv. Phys.* 62 (2013) 113-224.
- [156] Y. F. Guo, D. Q. Ye, K. F. Chen, J. C. He, and W. L. Chen, Toluene Decomposition Using a Wire-Plate Dielectric Barrier Discharge Reactor with Manganese Oxide Catalyst in Situ, *J. Mol. Catal. A Chem.* 245 (2006) 93-100.
- [157] X. Tu, H. J. Gallon, M. V. Twigg, P. A. Gorry, and J. C. Whitehead, Dry Reforming of Methane over a Ni/Al₂O₃ Catalyst in a Coaxial Dielectric Barrier Discharge Reactor, *J. Phys. D: Appl. Phys.* 44 (2011) 274007.
- [158] J. Van Durme, J. Dewulf, C. Leys, and H. Van Langenhove, Combining Non-Thermal Plasma with Heterogeneous Catalysis in Waste Gas Treatment: A Review, *Appl. Catal. B Environ.* 78 (2008) 324-333.
- [159] B. Eliasson, C. J. Liu, and U. Kogelschatz, Direct Conversion of Methane and Carbon Dioxide to Higher Hydrocarbons Using Catalytic Dielectric-Barrier Discharges with Zeolites, *Ind. Eng. Chem. Res.* 39 (2000) 1221-1227.
- [160] H. J. Gallon, X. Tu, and J. C. Whitehead, Effects of Reactor Packing Materials on H₂ Production by CO₂ Reforming of CH₄ in a Dielectric Barrier Discharge, *Plasma Process. Polym.* 9 (2012) 90-97.
- [161] K. Zhang, U. Kogelschatz, and B. Eliasson, Conversion of Greenhouse Gases to Synthesis Gas and Higher Hydrocarbons, *Energy Fuels* 15 (2001) 395-402.
- [162] K. Zhang, B. Eliasson, and U. Kogelschatz, Direct Conversion of Greenhouse Gases to Synthesis Gas and C₄ Hydrocarbons over Zeolite HY Promoted by a Dielectric-Barrier Discharge, *Ind. Eng. Chem. Res.* 41 (2002) 1462-1468.
- [163] T. Jiang, Y. Li, C. Liu, G. Xu, B. Eliasson, and B. Xue, Plasma Methane Conversion Using Dielectric-Barrier Discharges with Zeolite A, *Catal. Today* 72 (2002) 229-235.
- [164] D. Mei, B. Ashford, Y. L. He, and X. Tu, Plasma-Catalytic Reforming of Biogas over Supported Ni Catalysts in a Dielectric Barrier Discharge Reactor: Effect of Catalyst Supports, *Plasma Process. Polym.* 14 (2017) 1600076.

- [165] M. Zhu, A. Zhong, D. Dai, Q. Wang, T. Shao, and K. Ostrikov, Surface-Induced Gas-Phase Redistribution Effects in Plasma-Catalytic Dry Reforming of Methane: Numerical Investigation by Fluid Modeling, *J. Phys. D: Appl. Phys.* 55 (2022) 355201.
- [166] A. Bogaerts, X. Tu, J. C. Whitehead, G. Centi, L. Lefferts, O. Guaitella, F. Azzolina-Jury, H. Kim, A. B. Murphy, W. F. Schneider, T. Nozaki, J. C. Hicks, A. Rousseau, F. Thevenet, and A. Khacef, The 2020 Plasma Catalysis Roadmap, *J. Phys. D: Appl. Phys.* 53 (2020) 443001.
- [167] A. Indarto, Hydrogen Production from Methane in a Dielectric Barrier Discharge Using Oxide Zinc and Chromium as Catalyst, *J. Chin. Inst. Chem. Eng.* 39 (2008) 23-28.
- [168] O. Khalifeh, H. Taghvaei, A. Mosallanejad, M. R. Rahimpour, and A. Shariati, Extra Pure Hydrogen Production through Methane Decomposition Using Nanosecond Pulsed Plasma and Pt-Re Catalyst, *Chem. Eng. J.* 294 (2016) 132-145.
- [169] X.-S. Li, C. Shi, K.-J. Wang, X.-L. Zhang, Y. Xu, and A.-M. Zhu, High Yield of Aromatics from CH₄ in a Plasma-Followed-by-Catalyst (PFC) Reactor, *AIChE J.* 52 (2006) 3321-3324.
- [170] P. Kasinathan, S. Park, W. C. Choi, Y. K. Hwang, J. S. Chang, and Y. K. Park, Plasma-Enhanced Methane Direct Conversion over Particle-Size Adjusted MO_x/Al₂O₃ (M = Ti and Mg) Catalysts, *Plasma Chem. Plasma Process.* 34 (2014) 1317-1330.
- [171] S. Hu, B. Wang, Y. Lv, and W. Yan, Conversion of Methane to C₂ Hydrocarbons and Hydrogen Using a Gliding Arc Reactor, *Plasma Sci. Technol.* 15 (2013) 555-561.
- [172] M. Ghanbari, M. Binazadeh, S. Zafarnak, H. Taghvaei, and M. R. Rahimpour, Hydrogen Production via Catalytic Pulsed Plasma Conversion of Methane: Effect of Ni-K₂O/Al₂O₃ Loading, Applied Voltage, and Argon Flow Rate, *Int. J. Hydrogen Energy* 45 (2020) 13899-13910.
- [173] J. D. Holladay, J. Hu, D. L. King, and Y. Wang, An Overview of Hydrogen Production Technologies, *Catal. Today* 139 (2009) 244-260.
- [174] E. Tatarova, N. Bundaleska, J. P. Sarrette, and C. M. Ferreira, Plasmas for Environmental Issues: From Hydrogen Production to 2D Materials Assembly, *Plasma Sources Sci. Technol.* 23 (2014) 063002.
- [175] F. Geng, V. P. Haribal, and J. C. Hicks, Non-Thermal Plasma Assisted Steam Methane Reforming for Electrically-Driven Hydrogen Production, *Appl. Catal. A Gen.* 647 (2022) 118903.
- [176] T. Nozaki and K. Okazaki, Non-Thermal Plasma Catalysis of Methane: Principles, Energy Efficiency, and Applications, *Catal. Today* 211 (2013) 29-38.
- [177] H. Kabashima, H. Einaga, and S. Futamura, Hydrogen Generation from Water, Methane, and Methanol with Nonthermal Plasma, *IEEE Trans. Ind. Appl.* 39 (2003) 340-345.
- [178] S. Tiwari, A. Caiola, X. Bai, A. Lalsare, and J. Hu, Microwave Plasma-Enhanced and Microwave Heated Chemical Reactions, *Plasma Chem. Plasma Process.* 40 (2020) 1-23.
- [179] A. Bogaerts and E. C. Neyts, Plasma Technology: An Emerging Technology for Energy Storage, *ACS Energy Lett.* 3 (2018) 1013-1027.